A network diagram consisting of various sized light blue circles connected by thin white lines, set against a solid blue background. The circles vary in size and are scattered across the page, with some larger circles acting as hubs.

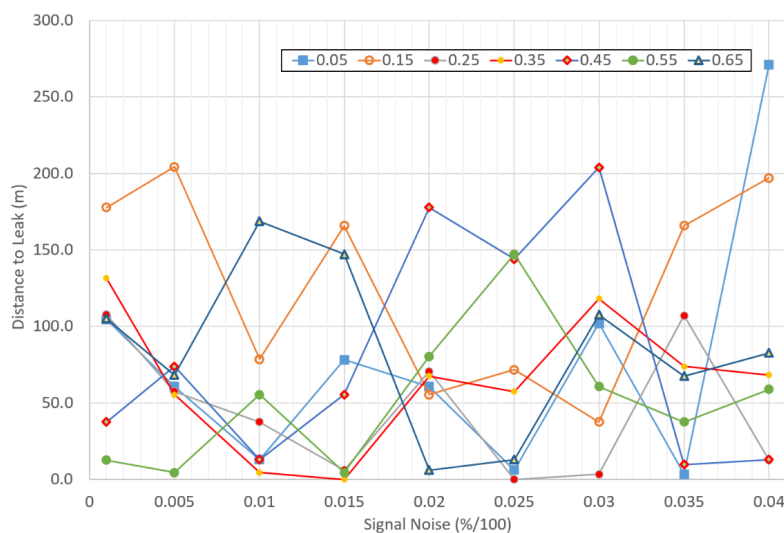
KWR 2021.001 | January 2021

**Callisto - Comparison  
and joint Application  
of Leak detection and  
Localization  
Techniques**

# Samenvatting

## Geavanceerde methoden voor lekdetectie en -lokalisatie ontsloten

Verlies van drinkwater dat uit distributiesystemen lekt, is wereldwijd een erkend probleem. Er bestaan reeds diverse methoden om lekken te detecteren en lokaliseren op basis van metingen van volumestroom en/of druk, soms in combinatie met hydraulische modellen. In de wetenschappelijke wereld worden bovendien regelmatig nieuwe algoritmen gepubliceerd. In dit project is een raamwerk gebouwd, in de vorm van een softwaretool, waarin verschillende methoden voor lekdetectie en -lokalisatie tegelijkertijd worden toegepast op volumestroom- en drukmetingen. Dit maakt het mogelijk om de prestatie van verschillende methoden te vergelijken (benchmarking), maar ook om de methoden in combinatie toe te passen en daarmee de eventuele zwakke plekken of blinde vlekken van individuele methoden te omzeilen. Succesvolle toepassing van de tool op praktijkdata wordt voorzien wanneer aan de twee randvoorwaarden wordt voldaan. Beide lijken haalbaar. Hiermee komt het effectief detecteren en lokaliseren op basis van diverse methoden uit de wetenschappelijke literatuur binnen handbereik van de drinkwaterbedrijven.



Afstanden tussen gesimuleerde lekken in een hydraulisch model en door Callisto teruggevonden locaties. In veel gevallen is deze minder dan 100 meter, ook in gevallen met veel ruis in de data. De verschillende kleuren representeren verschillende lekgrootten.

### Belang: van acceptatie naar aanpak van lekverliezen

Verlies van drinkwater dat uit distributiesystemen lekt, is wereldwijd een erkend probleem. Drinkwaterbedrijven hebben een scala aan redenen om ze aan te pakken. Voor Nederland lijken met name het mogelijke ontstaan van risicovolle situaties ten gevolge van lekken en de imago-driver van belang, in recente jaren ook gerelateerd aan optredende droogte; in het buitenland gelden ook financiële, ecologische en juridische drijfveren. Nederland heeft een goede staat van dienst op het gebied van

efficiënte drinkwaterdistributie. Maar ook hier zijn er gebieden met een verhoogd risico op lekkage. Er bestaan reeds diverse methoden om lekken te detecteren en lokaliseren op basis van metingen van volumestroom en/of druk, soms in combinatie met hydraulische modellen. In de wetenschappelijke wereld worden bovendien regelmatig nieuwe algoritmen gepresenteerd om lekkages op te sporen en te lokaliseren. Deze worden echter nog beperkt succesvol toegepast in de praktijk.

### **Aanpak: ontsluiting complementaire methoden in één tool**

Het doel van het project was om een raamwerk te bouwen waarin verschillende methoden voor lekdetectie en -lokalisatie tegelijkertijd worden toegepast op volumestroom- en drukmetingen. Hiervoor is een (onderzoeks)softwaretool ontwikkeld waarin verschillende lekdetectie- (namelijk VLPV/CFPD, Spectraalanalyse, Autoregressieanalyse en Support Vector Regressie) en leklokalisatie- (namelijk inversie van een hydraulisch model) technieken gecombineerd en met elkaar vergeleken kunnen worden. Het resultaat is een tool die aan de hand van tijdreeksen van volumestroom en druk, en in combinatie met een hydraulisch model, het mogelijk maakt om te bepalen of er al dan niet sprake is van een lek in een distributiegebied of DMA en wat de omvang en de waarschijnlijke locatie van het lek zijn. Bovendien kunnen andere bronnen van waterverlies (bv. diefstal, zeer relevant in sommige buitenlandse, en mogelijk administratieve verliezen als gevolg van fouten in de debietmeting in de uitgaande pijpleidingen van productielocaties of op DMA-grenzen) worden geïdentificeerd en gekwantificeerd. Er is bovendien een geavanceerde module voor datakwaliteitscontrole in de tool opgenomen, die veelvoorkomende datakwaliteitsproblemen identificeert en waar mogelijk verhelpt, voordat de daadwerkelijke lekanalyse wordt uitgevoerd. De tool maakt het mogelijk om de prestatie van verschillende methoden te vergelijken (benchmarking), maar ook om de methoden in combinatie toe te passen en daarmee de eventuele zwakke plekken of blinde vlekken van individuele methoden te omzeilen.

### **Resultaten: werking overtuigend aangetoond op synthetische lekken, inzichten opgedaan voor praktijktoepassing**

De tool is getest met synthetische data (in de computer gesimuleerde lekken) en met in het veld gesimuleerde lekken (spuitests) in twee verschillende DMA's in Nederland. Dit heeft voor synthetische lekken aangetoond dat de tool correct functioneert en in staat is om het juiste gebied voor de lekkages aan te geven (meestal binnen 100-200 meter van het werkelijke lek). Dit geldt ook voor significante ruisniveaus in de tijdreeksen (tot 10%), die kunnen worden beschouwd als representatief voor zowel onzekerheden in de metingen als de effecten van de stochastische watervraag. De toepassing van de tool op data van spuitests in het veld is in eerste instantie minder succesvol gebleken, maar de hieruit voortkomende inzichten bieden veel perspectief voor succesvolle veldtoepassing.

Het basisprincipe van de Callisto-tool is dat een combinatie van methoden resulteert in een groter vertrouwen in de daadwerkelijke opsporing van lekken. Dit is tot nu toe niet onomstotelijk aangetoond, maar de voorlopige analyse die in dit rapport wordt gepresenteerd suggereert wel een toegevoegde waarde in de gecombineerde toepassing van meerdere methoden.

### **Toepassing: hordes voor de praktijk zijn te nemen**

Succesvolle toepassing van de tool op praktijkdata wordt voorzien wanneer aan de volgende randvoorwaarden wordt voldaan: 1) Voor het opsporen van lekken dient een grondige analyse uit te worden gevoerd die zowel de timing als de omvang van de lekken vaststelt. De eerste wordt geïdentificeerd door alle geïmplementeerde methoden, de tweede in het bijzonder ook door VLPV/CFPD (Vergelijking van leveringspatroonverdeling, Comparison of Flow Pattern Distributions) en spectrale analyse. 2) Voor de lokalisatie van lekken dient te worden gezorgd dat het gebruikte hydraulische model voldoende representatief is voor de werkelijke hydraulische omstandigheden in het veld, zowel in termen

van topologie/connectiviteit als in het bijzonder ook in termen van de watervraag. Beide aspecten zijn haalbaar. Hiermee komt het effectief detecteren en lokaliseren op basis van diverse methoden uit de wetenschappelijke literatuur binnen handbereik van de drinkwaterbedrijven.

## Collaborating Partners



# Report

## Callisto - Comparison and joint Application of Leak detection and Localization Techniques

KWR 2021.001 | January 2021

### Project number

402518

### Project manager

drs. P.G.G. (Nellie) Slaats

### Author(s)

M. (Mario) Castro Gama MSc, J.W. (Hans) Zijlstra MSc

### Quality Assurance

dr. E.M.J. (Mirjam) Blokker, dr.ir. A.C. (Arie) de Niet

### Sent to

This report was distributed among all project partners. The report is public.

This activity is co-financed with PPS-funding from the Topconsortia for Knowledge & Innovation (TKI's) of the Ministry of Economic Affairs and Climate. Procedures, calculation models, techniques, designs of trial installations, prototypes and proposals and ideas put forward by KWR, as well as instruments, including software, that are included in research results are and remain the property of KWR, with the exception of the Dataprofeet module, which is and remains the property of Witteveen+Bos Consulting Engineers (W+B). All rights arising from KWR's and W+B's intellectual and industrial property, as well as associated copyrights, also remain with KWR and W+B and therefore the property of KWR and W+B, respectively.

### Keywords

leak detection, leak localization

[Year of publishing](#)  
2021

### More information

dr. P. (Peter) van Thienen  
T 030 6069 602  
E [peter.van.thienen@kwrwater.nl](mailto:peter.van.thienen@kwrwater.nl)

PO Box 1072  
3430 BB Nieuwegein  
The Netherlands

T +31 (0)30 60 69 511  
E [info@kwrwater.nl](mailto:info@kwrwater.nl)  
I [www.kwrwater.nl](http://www.kwrwater.nl)

**KWR**

**Witteveen + Bos**

January 2021 ©

All rights reserved by KWR. No part of this publication may be reproduced, stored in an automatic database, or transmitted in any form or by any means, be it electronic, mechanical, by photocopying, recording, or otherwise, without the prior written permission of KWR.

# Contents

<b>Samenvatting</b>	<b>1</b>
<b>Collaborating Partners</b>	<b>4</b>
<b>Report</b>	<b>5</b>
<b>Contents</b>	<b>6</b>
<b>1 Introduction</b>	<b>8</b>
1.1 Background and context	8
1.2 Project objective and tool development	8
1.3 Consortium	9
1.4 Project team	9
1.5 How to read this report	10
<b>2 Literature on leak detection and localization</b>	<b>11</b>
2.1 Approach	11
2.2 Method types by use of software or hardware	12
2.3 Categories of modeling techniques for different methods	12
2.4 Pre-screening of methods for leak detection	13
2.5 Practical aspects of implementation of Callisto	13
<b>3 Selected methods</b>	<b>15</b>
3.1 Introduction	15
3.2 Leak detection methods	15
3.2.1 CFPD	15
3.2.2 AUTOREGRESSIVE MODEL	17
3.2.3 SPECTRAL ANALYSIS	19
3.2.4 SUPPORT VECTOR REGRESSION	20
3.3 Leak Localization method	21
3.4 Data Quality Control - Dataprofeet	21
3.4.1 Chronology	21
3.4.2 Missing	21
3.4.3 Bad / dead signal	21
3.4.4 Not A Number (NaN)	22
3.4.5 Linear trend	22
3.4.6 Step trend	23
3.4.7 Double date	24
3.4.8 Interpolated	24
3.4.9 Outlier Daily	24
3.4.10 Outlier Spike	25

<b>4</b>	<b>Callisto tool</b>	<b>28</b>
<b>5</b>	<b>Case studies</b>	<b>29</b>
5.1	Selection of case studies	29
5.2	Historical records	29
5.3	Flushing tests	30
5.4	Data of time series of flushing tests.	30
5.5	Execution of flushing tests	31
<b>6</b>	<b>Results</b>	<b>33</b>
6.1	Introduction	33
6.2	Method and sensitivity testing on synthetic data	33
6.3	Flushing experiments - Duindorp	34
6.3.1	Leak detection	34
6.3.2	Leak Localization	35
6.3.3	True characteristics of flushes and failure analysis	35
6.4	Flushing experiments in Diemen-Noord	37
6.4.1	Leak detection	37
6.4.2	Leak localization	40
6.4.3	True characteristics of flushes and analysis	40
6.5	Additional a posteriori analyses	42
6.5.1	Localization of simulated leaks in Duindorp	42
6.5.2	Localization of simulated leaks in Diemen-Noord	43
<b>7</b>	<b>Conclusions and recommendations</b>	<b>44</b>
7.1	Conclusions	44
7.2	Recommendations	44
<b>8</b>	<b>Bibliography</b>	<b>46</b>
<b>I</b>	<b>Appendix: Flushing plan and proposed leakage locations to water companies.</b>	<b>49</b>



# 1 Introduction

## 1.1 Background and context

Loss of drinking water leaking from distribution systems is a recognised problem worldwide. Drinking water companies have a range of drivers to address them. For the Netherlands, the prevention of potentially risky situations caused by leaks and the image driver seem particularly important; abroad, financial, ecological and legal drivers also apply. The Netherlands has a good track record in the field of efficient drinking water distribution. But here, too, there are areas with an increased risk of leakage. New algorithms are regularly presented in the scientific world to identify and localise leaks.

In addition to traditional methods for identifying leakage losses (e.g. using the AWWA water balance), there are various quantitative approaches for identifying leakage losses and changes in leakage volumes, suitable for different spatial and temporal scales. Examples include Minimum Night Flow, CFPD (Comparison of Flow Pattern Distributions) and dynamic bandwidth monitor, with various filter techniques etc. All methods have their advantages and disadvantages, and for the time being there is no method that performs optimally under all circumstances (area size, size and types of leaks, variation in the consumption signal, etc.); i.e. detects all leaks (no false negatives) and classifies events that are not leaks as such (no false positives). Presumably, different methods are complementary, and a combination of methods offers perspective for avoiding false positive and false negative determinations. What is currently lacking, however, is a framework to apply different methods side by side - complementary - for comparison and to increase the yield of the analysis.

## 1.2 Project objective and tool development

The objective of the project was to build a framework in which existing methods are simultaneously applied to flow and pressure measurements. For this purpose, a (research) tool was created in which various leak detection and leak localisation techniques can be combined and compared with each other. The result is a tool which, on the basis of time series of flow and pressure, and in combination with a hydraulic model, makes it possible to determine whether or not there is a leak in the area, the size of the leak, and the probable location of the leak. In addition, other sources of water loss (e.g. theft, very relevant in some foreign countries, and perhaps administrative losses due to flow metering errors in outgoing pipelines from production sites or at distribution area boundaries) can be identified and quantified. This can also provide insight into the desired size of a measurement area or DMA (district metered area, a distinct part of the network, generally of limited size with some thousands of connections, for which all incoming and outgoing flows are measured, so that a water balance can be determined). No requirements for detectable leakage sizes were defined at the outset. This is quite difficult, since this depends on the analysis methods, the type and number of sensors used, and in particular also on the characteristics of the DMA or supply area itself.

On the basis of the modelling possibilities the water companies can assess whether the current division into DMAs matches the leaks they hope to find, or whether they need to reduce their DMAs. Pressure measurements at customers' premises (smart water meters that also measure pressure) may also be useful.

The tool has been applied to two distribution areas with different characteristics (including size), using experimental data, for validation purposes. An additional objective was to investigate whether this indeed leads to fewer false negatives (a single method may miss a deviation such as a leak, a whole set of methods may lead to an alarm) or to fewer false positives (normal variation leads to an alarm in some methods, but a set of methods may

be able to assess that there is no deviation, but that it falls within the expected bandwidth). That secondary objective has not been completed because of constraints on the available data and field tests.

The tool differs from other commercially offered tools in that it is not based on a single analysis method with the additional limitations, but combines the strengths of different methods and complements their weaknesses. In addition, the presence of multiple methods ensures a broader usability, also for water companies that have limited amounts of data at their disposal. Moreover, the tool provides a framework for quantitatively determining how well methods or combinations of methods work.

The tool is named *Callisto: Comparison and joint Application of Leak detection and Localization Techniques*.

### 1.3 Consortium

The consortium consists of 4 partners (see Figure 1): two utilities (Dunea and Waternet), one industrial partner (Witteveen+Bos Consulting Engineers) and one research institute (KWR Water Research Institute).

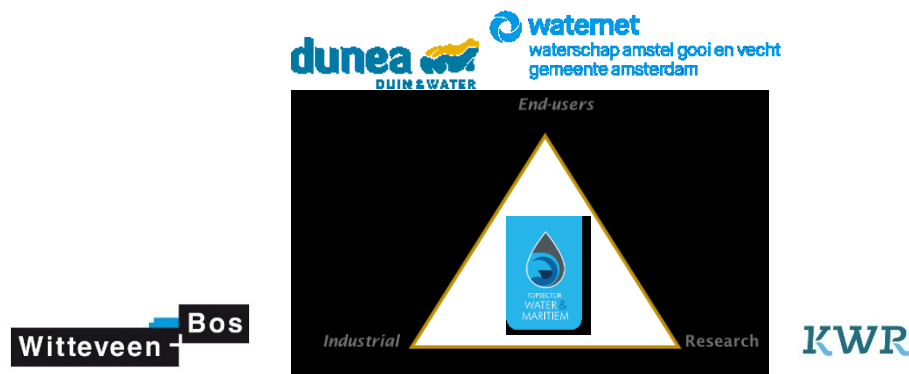


Figure 1. TKI Callisto CONSORTIUM

The utilities have shared their drinking water distribution network models and historical records of different systems and performed a set of flushing tests in the field. The industrial partner helped with the software development, while KWR developed the software implementation of selected methods for leak detection and localization.

### 1.4 Project team

The project team consisted of the following people in the following roles:

Mario Castro Gama	(KWR)	: testing, reporting, coding
Mark Morley	(KWR)	: tool development
Claudia Quintiliani	(KWR)	: user manual
Bram Hillebrand	(KWR)	: coding
Derk Rouwhorst	(WMD, seconded to KWR)	: coding
Nellie Slaats	(KWR)	: project management
Peter van Thienen	(KWR)	: lead researcher, final editing of the report
Mirjam Blokker	(KWR)	: quality assurance
Michel Bretveld	(Witteveen+Bos)	: lead researcher for W+B
Hans Zijlstra	(Witteveen+Bos)	: coding, testing, reporting
Arie de Niet	(Witteveen+Bos)	: quality assurance
Sil Nieuwhof	(Witteveen+Bos)	: coding, testing

Arne Bosch (Waternet) : end user project steering, field test organization  
Michael van den Boom (Dunea) : end user project steering, field test organization

## **1.5 How to read this report**

This document presents the main stages of Callisto development, from literature to tool testing. It includes the results of the tests on the case studies. Chapter 2 provides an overview of the literature on leak detection and localization methods. The methods that have been selected for inclusion in the Callisto tool are discussed in Chapter 3; the tool itself is briefly introduced in Chapter 4. This is followed by a description of the case studies in Chapter 5 and analysis results for these in Chapter 6. The report ends with a discussion, conclusions, and recommendations in Chapter 7.

## 2 Literature on leak detection and localization

### 2.1 Approach

Initially, a large literature search was performed on leak detection and leak localization techniques, finding more than 120 papers. From this collection, it was evident that a subset of techniques (or variations on these) are actually feasible for implementation and simultaneously have been tested on both synthetic and field measurements data.

Various authors have done a literature review before us. We have happily made use of their efforts. Fourteen literature reviews on different aspects of leak detection and leak localization (see Table 1) were scrutinized to identify the best combination of methods and its accuracy. Most of the reviews focus on numerical/computational aspects of algorithms, while the reviews of van Vossen-van den Berg, (2017), EU (2015), and Mesman & van Thienen (2015) refer to the combination with practical aspects. Based on these reviews, a suitable set of methods was proposed by KWR and agreed upon by the project partners.

*Table 1. A collection of literature review concerning leakage quantification, detection and localization.*

<i>Reference</i>	<i>Title</i>	<i>Type</i>
Van Vossen-Van den Berg, 2017	Overview and application of leak localization techniques (Overzicht en toepassing van lekopsporingstechnieken)	Overview
Wu & Liu, 2017	A review of data-driven approaches for burst detection in water distribution systems	Review
Berardi & Giustolisi, 2016 Giustolisi, Berardi, Laucelli, Savic, & Kapelan, 2016	Special Issue on the Battle of Background Leakage Assessment for Water Networks	Competition of model-based methods
Mesman & van Thienen, 2015	Leak localization using hydraulic models (Lekzoeken met hydraulische modellen)	Overview
EU, 2015	Reference Document Good Practices on Leakage Management WFD CIS WG PoM	Best Practices
Hutton, Kapelan, Vamvakieridou-Lyroudia, & Savić, 2014	Dealing with uncertainty in water distribution system models: a framework for real-time modeling and data assimilation	Review
Li, Huang, Xin, & Tao, 2014	A review of methods for burst/leakage detection and location in water distribution systems	Review
Mutikanga, Sharma, & Vairavamoorthy, 2013	Methods and Tools for Managing Losses in Water Distribution Systems	Review
Puust, Kapelan, Savic, & Koppel, 2010	A review of methods for leakage management in pipe networks	Review
Colombo, Lee, & Karney, 2009	A selective literature review of transient-based leak detection methods	Review
Geiger, 2006	State of the Art in Leak Detection and Localisation	Review
Alegre, et al., 2006	(performance Indicators for Water Supply Services (Manual of Best Practice)	Best Practices (NRW)
Buchberger & Nadimpalli, 2004	Leak Estimation in Water Distribution Systems by Statistical Analysis of Flow Readings	Review

NRW: Non-revenue water

## 2.2 Method types by use of software or hardware

In the set of methods presented in the reviews (, a suitable set of methods was proposed by KWR and agreed upon by the project partners.

Table 1) a distinction can be made between two types of leak detection and localization methods: software based and hardware based methods. Callisto focuses on software based methods. An overview of method classes is provided in Table 2.

For software based methods, the following observations can be made:

- 1) In general terms, it is often required to define thresholds in a subjective or analytical form to determine when there is an occurrence of burst or background leakage. Such thresholds are based on historical records, others may be derived from model simulations.
- 2) The data or some derivative of these are compared to threshold values.

*Table 2. Hardware and software based leak detection and localization methods.*

Type	Sub-type	Methods	Shared characteristics
Software based methods	Model-based	<ul style="list-style-type: none"> <li>• Hydraulic modeling</li> <li>• Transients</li> <li>• Time decomposition</li> <li>• Frequency domain</li> </ul>	<ul style="list-style-type: none"> <li>• Detect and locate the leakage timely and accurately</li> <li>• Determine the possible leakage are; cannot locate the leakage point precisely</li> <li>• Application of more sophisticated algorithms and principles needed</li> <li>• Low cost in an extended horizon</li> </ul>
	Data-driven	<ul style="list-style-type: none"> <li>• Artificial Neural Network</li> <li>• Bayesian Inference</li> <li>• Kalman filter and variations</li> </ul>	
Hardware based methods	Acoustic	<ul style="list-style-type: none"> <li>• Listening rods</li> <li>• Correlators</li> <li>• Noise loggers</li> <li>• Inspection tool mounted hydrophones</li> </ul>	<ul style="list-style-type: none"> <li>• Pinpoint the location of leakage</li> <li>• Labor intensive and requires scheduling</li> <li>• Applies to leakage detection of a small range</li> <li>• Generally high cost in an extended horizon</li> </ul>
	Non-acoustic	<ul style="list-style-type: none"> <li>• Gas injection</li> <li>• Ground penetrating radar</li> </ul>	

## 2.3 Categories of modeling techniques for different methods

Modeling techniques for leak detection and localization can be data-driven (including statistical) or based on hydraulic models. There are three categories of data-driven modeling techniques (either for burst or background leakage), originating from different data mining and modeling methods:

- statistical: using classical statistics to describe and distinguish features;
- classification: identifying the plausibility of a leakage or burst;
- prediction-classification: making a comparison between a hydraulic model and a data-driven model, or using a forecast window.

Table 3 presents a set of advantages and limitations for each category.

Table 3. Different categories of methods with limitations and advantages, based on the reviews listed in Table 1.

Category	Advantages	Limitations and challenges
Classification	<ul style="list-style-type: none"> <li>• With small number of classes and visualization it is meaningful to operators</li> <li>• Easy to implement, and ready to use in many software libraries</li> </ul>	<ul style="list-style-type: none"> <li>• Usually hydraulic data contains no labels to train and test models</li> <li>• Unbalanced classes affect classification during testing</li> <li>• Classes cannot be dynamically updated, meaning that also new events belonging to a class that was not observed before will be classified in of the existing classes.</li> </ul>
Prediction-classification	<ul style="list-style-type: none"> <li>• The combination of prediction and classification improves the identification</li> <li>• It is possible to deal with uncertainty better than with other methods</li> <li>• Gives insights of deviation from trend or pattern and how far away prediction is from observation</li> <li>• Can be used to feedback information to update model</li> </ul>	<ul style="list-style-type: none"> <li>• Propagation of uncertainty in long-term predictions</li> <li>• Depending on complexity it may become computationally cumbersome</li> <li>• Misleading results can be obtained when the stochastic nature of parameters (in particular demand) is not taken into account.</li> <li>• The hydraulic model should produce output that is adequately representative of the real system</li> </ul>
Statistical	<ul style="list-style-type: none"> <li>• Computationally lightweight</li> <li>• Easy to implement</li> </ul>	<ul style="list-style-type: none"> <li>• Inappropriate probability density function assumptions bias the estimation</li> <li>• Definitions of thresholds require expert knowledge and does not guarantee identification</li> </ul>

## 2.4 Pre-screening of methods for leak detection

Based on the literature review a number of methods was preselected (see Table 4). These were discussed in a meeting with the project partners to decide which methods to implement in the Callisto tool. The main criteria considered for the selection of methods for implementation in Callisto are:

- Number of sensors required, because utilities prefer to minimize the number of sensor installations. The range is wide with methods that consider only one sensor signal (Eliades & Polycarpou, 2012, van Thienen & Vertommen, 2015) to methods with hundreds of sensors (Mounce, Mounce, & Boxall, 2011).
- Leak magnitude & percentage of total inflow. It is important to be able to emulate the behavior of different leakages also if they correspond to a low percentage of the total inflow or if the leakages are equivalent to 100% of the total inflow (Mounce & Machell, 2006).
- Required data resolution to match that available at the water companies participating in the project.

## 2.5 Practical aspects of implementation of Callisto

Callisto is intended to increase the capacity of the operators to detect and locate leakages. This refers both to immediate events (bursts) and leakages that have been undetected for a longer time (unreported/background leakage). Localization means to identify the area of pipe where a leakage is most likely to occur. A perfect (but in practice not available) algorithm would be able to pinpoint exactly the pipe(s) where the leakage(s) is (are) located in a drinking water distribution network. The more realistic aim set for Callisto is to identify a set of possible leak locations, in order to narrow down the search area(s) for the field operators.

Table 4. List of pre-screened methods for Callisto development. Bold-faced methods have been selected for inclusion in the Callisto tool, see Chapter 3.

Reference	Technique/Method	Category *	Case study	Lead Time	Leakage magnitude or percentage	Number of Sensors	Data type	Resolution Measurements
Housh & Ohar, 2018 Housh & Ohar, 2017	Moving Average (MA), with parameters calibrated using CANARY from (U.S.-EPA, 2012)	PC	Benchmark C-Town	Uses offline data	Min 108 m <sup>3</sup> /h (15%)	47	Flow / Pressure	15 min
(Bakker, Vreeburg, Roer, & Rietveld, 2014, Bakker, 2014)	Adaptive Forecasting	PC	Several DMA's in NL	Window of 1 week. In small systems 30 min	7-150 m <sup>3</sup> /h (22 – 6.5%)	1/9 for the largest DMA	Flow/Pressure	15 min (forecast)
<b>Eliades &amp; Polycarpou, 2012</b>	<b>Spectral (Fourier) and CUSUM (cumulative sum)</b>	PC	Limassol, Cyprus	<b>Approx. 12 days</b>	<b>0.5 – 3.0 m<sup>3</sup>/h (4%)</b>	<b>1 time series analysed</b>	<b>Flow</b>	<b>5 min</b>
<b>Mounce, Mounce, &amp; Boxall, 2011</b>	<b>Support Vector Regression (SVR)</b>	PC	<b>The Harrogate and Dales (H&amp;D), UK</b>	<b>12 h window, with constant update</b>	<b>65 m<sup>3</sup>/h (~100%)</b>	<b>450 loggers 412 flows and pressures</b>	<b>Flow / Pressure</b>	<b>15 min</b>
Ye & Fenner, 2010	Extended Kalman Filter	PC	Several DMA's North UK	15 min, Kalman update	7-18 m <sup>3</sup> /h (10-25%)	1/1	Flow / Pressure	1 min & 15 min
Caputo & Pelagagge, 2003 Caputo & Pelagagge, 2002	Artificial Neural Network (ANN)	PC	Benchmark of 13 pipes	1 time step, but requires prior training	32-160m <sup>3</sup> /h (2-10% of flow rate)	1 / 29 (all nodes)	Flow / Pressure	N/A
Romano, Woodward, & Kapelan, 2017 Romano, Kapelan, & Savic, 2014	Statistical Process Control	S	Several DMA's in UK. Only results for 1 are shown.	Undisclosed	1-7m <sup>3</sup> /h (1-40%) flow DMA's. 6% presented.	5 / 6	Flow/Pressure	1 min
<b>Van Thienen (2013)</b> (van Thienen & Vertommen, 2015)	<b>Comparison of Flow Pattern Distributions (CFPD)</b>	S	<b>Synthetic generated based on real data, several DMAs in Paris</b>	<b>Uses offline data</b>	<b>5-10m<sup>3</sup>/h (6-16%)</b>	<b>1 per time series</b>	<b>Flow</b>	<b>Different resolutions</b>
Palau, Arregui, & Carlos, 2012	Principal Component Analysis and statistics	S	Undisclosed DMA in Spain	Function of the hour of the day and leak size	13 m <sup>3</sup> /h (5%)	1	Flow	1 hour
<b>Wang, Dong, &amp; Fang, 1993</b>	<b>Autoregression (AR)</b>	S	<b>A 10mm pipe of 120 m length</b>	<b>Given by autoregression</b>	<b>undisclosed (1-2% flow, 0.5% pressure)</b>	<b>4</b>	<b>Pressure</b>	<b>20 ms</b>
Aksela, Aksela, & Vahala, 2009	Artificial Neural Network with Self-Organizing Map (ANN with SOM)	C	Undisclosed	Requires data up to 100 days for forecast	Up to 100m <sup>3</sup> /h Low threshold undisclosed	3	Flow	1 hour
Mounce & Machell, 2006	Artificial Neural Network (ANN) with time delay	C	DMA in UK	Offline data	11 m <sup>3</sup> /h (100%)	3/3	Flow / Pressure	15 min
Wu et al. (2010)	inversion of hydraulic model using genetic algorithm	HM	a 840 node network in the UK				Flow / Pressure	
Meseguer et al. (2014)	model based leakage signature database	HM	a 1996 node network in Barcelona				flow/pressure	

\*P: prediction, PC: prediction-classification, S: statistical, HM: hydraulic model-based

## 3 Selected methods

### 3.1 Introduction

During a dedicated meeting in December 2018, and based on the list of techniques (see Table 4) four algorithms were selected. They represent a range of different, and therefore potentially complementary, methods that have feasible data requirements and acceptable detection limits. Furthermore, one of them was developed by KWR and code had already been developed for a second as well.

For leak detection a selection of four algorithms was made:

- Comparison of Flow Pattern Distributions (CFPD) (van Thienen & Vertommen, 2015);
- Support Vector Regression (SVR) (Mounce et al., 2011);
- Statistical Autoregressive (AR) (Wang, Dong, & Fang, 1993).
- Spectral Analysis (SA) (Eliades & Polycarpou, 2012).

For leak localization, the following method was selected:

- Hydraulic Based Inverse Modelling (Wu et al., 2010).

These methods are described in more detail in sections 3.2 and 3.3.

Prior to the actual analysis of the data, some quality control and cleaning up of the data may be required. A specialized module based on Witteveen+Bos' Dataprofeet was included for that purpose. This is described in section 3.4.

### 3.2 Leak detection methods

#### 3.2.1 CFPD

The Comparison of Flow Pattern Distributions was introduced in 2013 (Van Thienen, 2013). This section presents the summary of the method that was published in Van Thienen et al. (2015).

Consider a supply area for which the flow rate into the area (accounting for all inflow, outflow and storage) is registered for a period of time (e.g. a day, a week, a month or an entire year) and again for a comparable period of the same length in another year. The registered patterns are likely to be similar in shape but not exactly the same. The simple CFPD procedure allows a quantitative comparison of these patterns, taking the following steps:

1. Sort both data sets from small to large magnitude. Sorted measurement ranks, scaled to a 0-1 range, are on the horizontal axis, flow rates are on the vertical axis.
2. Plot one data set against the other in a CFPD plot.
3. Determine a linear best fit with slope  $a$  and intercept  $b$ .

Note that the word pattern is used here in the sense of a time series which is generally repetitive to a significant degree with some variations. In general, it is preferable to construct the CFPD plot with the first period on the horizontal axis and the second on the vertical. In this case  $a > 1$  and/or  $b > 0$  corresponds to an increase in flow rate. Note that comparison of periods of different length is also possible but requires an additional interpolation step, see Van Thienen (2013).

For the application of the CFPD procedure on long time series, it is desirable to perform a comparison of each period (which will be called block in the following) within this time series with each other period. This allows the identification of changes on the timescale of individual blocks.



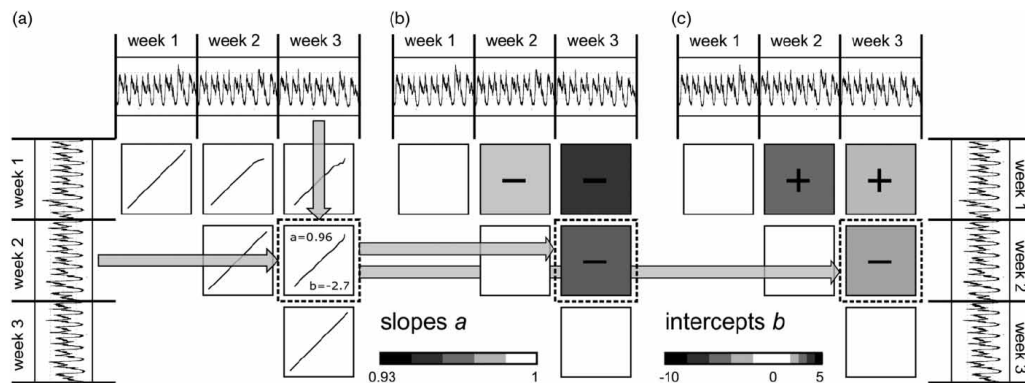


Figure 2 illustrates the procedure and results of such a block analysis. A CFPD analysis is made (Figure 2a) of all possible combinations of time blocks of a preselected length of the comparison frame within the complete dataset. Two matrices A (Figure 2b) and B (Figure 2c) are made, in which row  $i$  and column  $j$  represent blocks  $i$  and  $j$  (within the time series), respectively, and entries  $A_{ij}$  and  $B_{ij}$  are the factors  $a$  and  $b$ , respectively, resulting from a CFPD comparison of block  $i$  with period  $j$ . The entries in the upper triangle (the lower triangle is not shown, as the matrices are antisymmetric) are grey toned or coloured as a function of their deviation from 1 (A) and 0 (B), respectively, with small deviation having a light tone close to white and larger deviations having either a darker tone and a sign (-/=/+ ) indicating the direction of the deviation, or a red (+) or blue (-) colour. The complete matrices are constructed because it is usually not clear beforehand which time block is suitable as a reference time block.

Changes in  $a$  or  $b$  which remain in the signal longer than the frame length will show up in the block analysis as blocks of similar tone and sign, allowing direct pinpointing (in time) of events which cause these changes, see Figure 3. Changes in  $a$  (called *consistent changes*) may represent changes in behaviour, population size, water theft., etc. Changes in  $b$  (called *inconsistent changes*) may represent leakages, flushing, and valve manipulations. Note that when the fit is bad, i.e. the data do not conform well to the conceptual model of CFPD, the standard deviation of the fit is large. This means that the results should be interpreted with caution. This happens in particular when events have a duration smaller than the length of an individual block in the analysis.

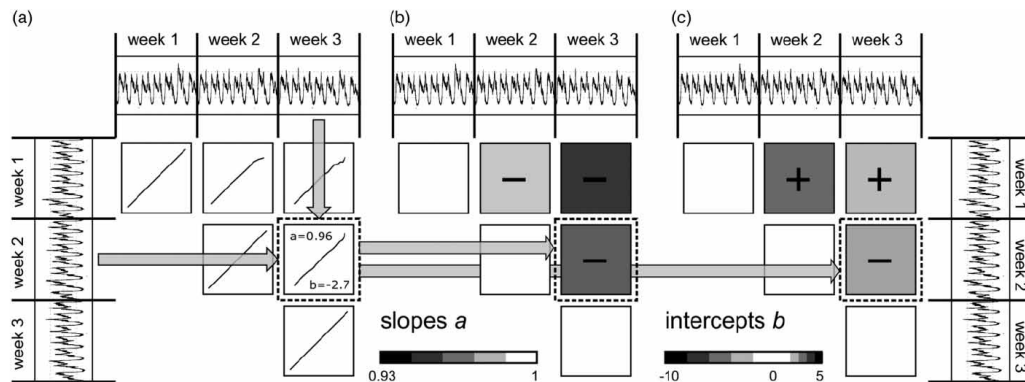


Figure 2. Illustration of the CFPD block analysis. a) CFPD analysis for each combination of blocks, b) visualization of slope values (matrix A), c) visualization of intercept values (matrix B). Copied from Van Thienen et al. (2013).

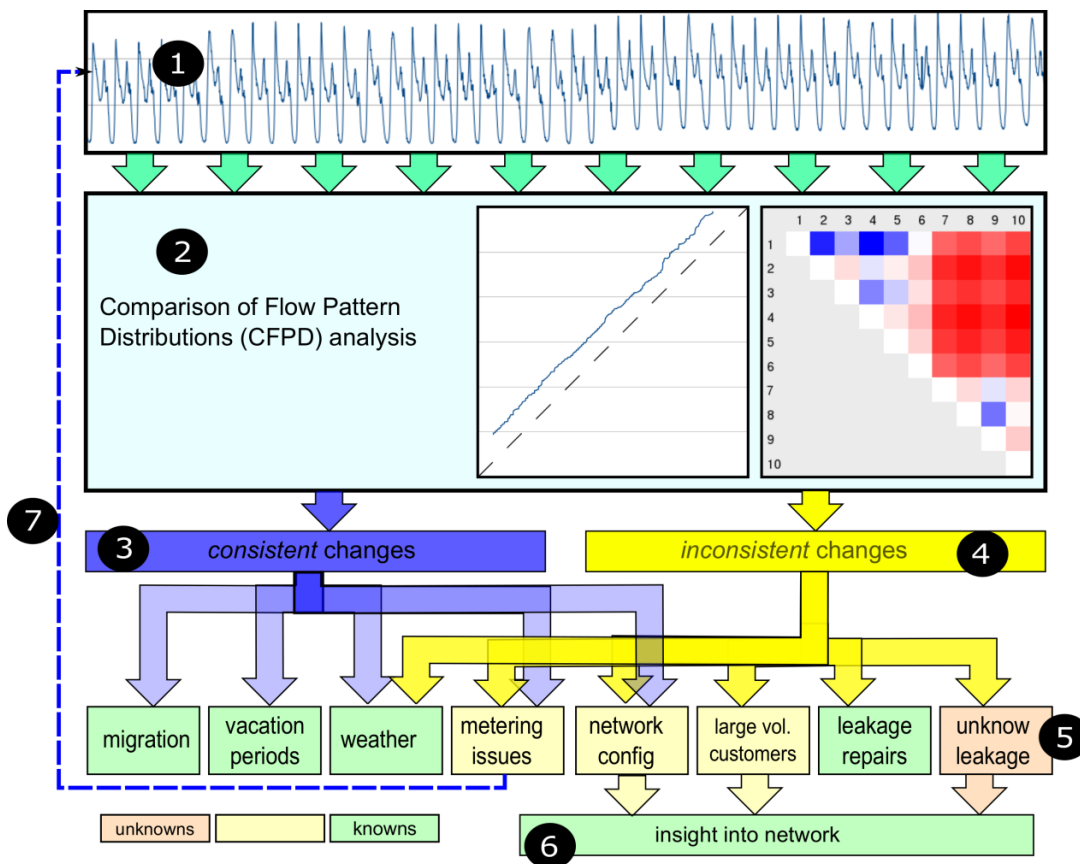


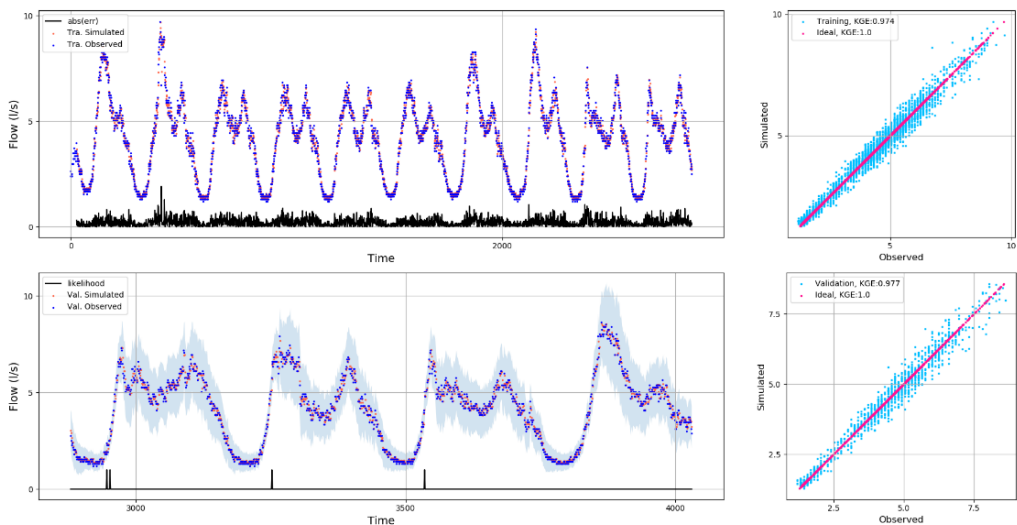
Figure 3: CFPD analysis procedure and interpretation. 1) flow time series; 2) CFPD analysis; 3,4) identification of consistent and inconsistent changes; 5) interpretation of these changes in terms of known and unknown mechanisms; 6) discarding changes by known mechanisms such as vacation periods, weather, among others, results in a reduced list of unknown events that can be responsible for the change, making the interpretation easier; 7) any data quality issues which are found may initiate improvement measures. Copied from Van Thienen and Vertommen (2015).

What the user of Callisto receives are the slopes, intercepts and errors for each of the comparisons, i.e. the block diagrams for slope, intercept and standard deviation (as shown schematically in Figure 2 and functionally in Figure 3). Changes represented as blue signify an increase in the variable with respect to other time windows, while values of red represent a decrease in the variable. For example in two consecutive weeks, where the second week presents a leakage the slope is expected to be red during the second week.

### 3.2.2 AUTOREGRESSIVE MODEL

The autoregressive model is a simple time series regression model based on correlation statistics on prior time steps. It builds a linear regression model based on the history of previous observations called lags and then

forecasts the time series into the future. For example an autoregressive model is presented for a input flow time



series in

Figure 4. It depicts the training (Tra) and Validation (Val). In this case 10 days are used for training and four days are used for validation. The time series resolution is 5 minutes, this gives a total number of validation timestamps (nval) of 1152. A significance level  $\alpha = 0.65$  is selected. The confidence interval is built for  $1 - \alpha$ . The top-left shows the training observed values and simulated showing good correspondence. The corresponding absolute error is presented, it demonstrates that even during training the largest errors correspond to timestamps where larger consumptions appear.

In order to determine the quality of the adjustment several metrics can be used: Mean Squared Error (MSE), correlation (r), coefficient of determination ( $R^2$ ), Nash-Sutcliffe Efficiency (NSE) or Kling-Gupta Efficiency (KGE). In this particular case

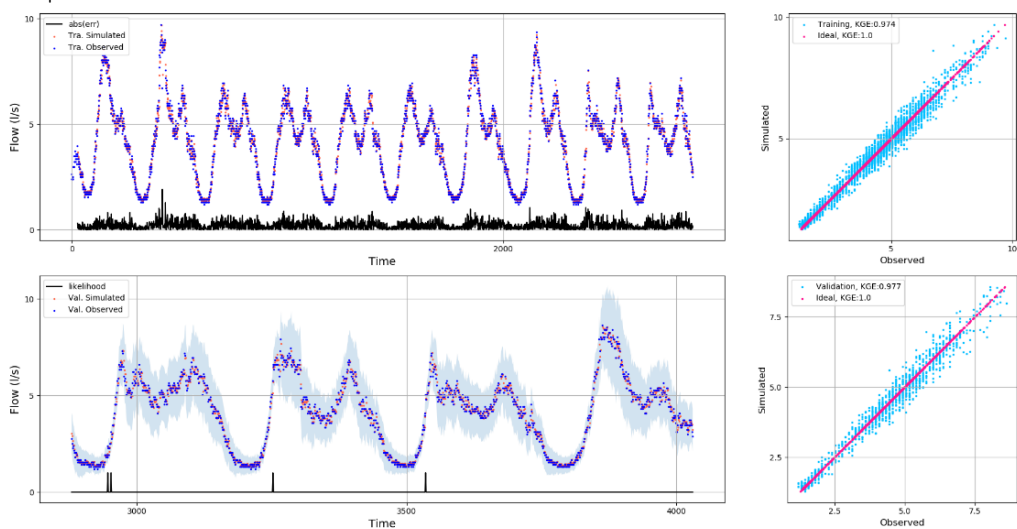


Figure 4 top-right and bottom-right, the adjustment is presented using KGE which must be close to 1.0 to emulate good fitness. This metric has been used in the example. As presented for both training and validation show KGE above 0.97.

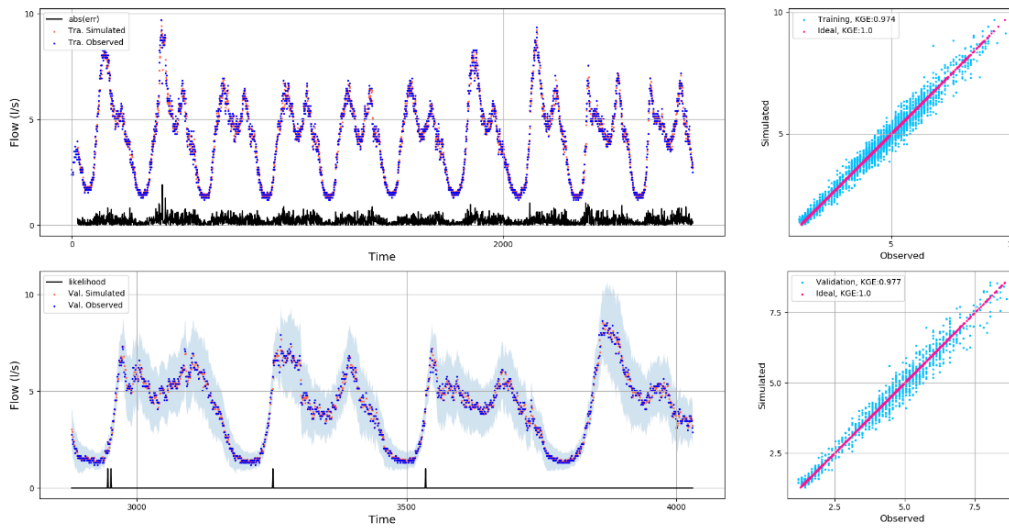


Figure 4. Autoregressive model of a 2 week time series of flows. Ten days are used for training and four days for validation. The right hand side plots also show data in l/s.

Figure 4 bottom left shows the confidence interval  $1-\alpha = 0.35$  (shaded area) of the validation. If the observed values fall within the confidence interval boundaries then no anomaly is detected, while if the opposite occurs then the likelihood increases. If consecutive timestamps show detection as anomaly then the likelihood increases linearly. Specifically in the case that the value of  $\alpha$  is changed the number of anomalies increases or decreases. For example, for the same time series of

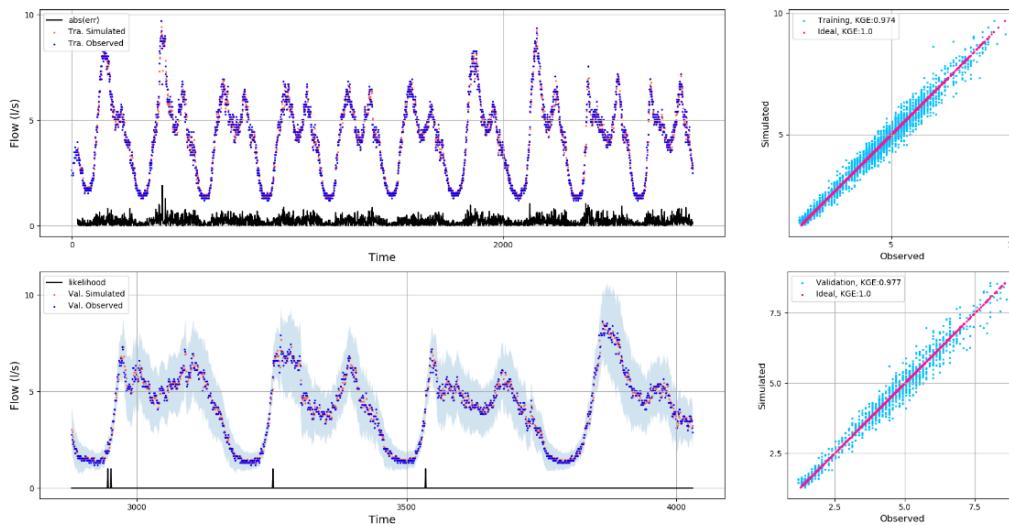


Figure 4, when changing the value of  $\alpha$  to 0.90 and 0.05 two different results are obtained as presented in Figure 5. If the value of  $\alpha$  is small (say 0.05) then the confidence interval is wide and no anomalies are detected. On the other hand if the value of  $\alpha$  is large (say 0.90) then the confidence interval is narrow and almost all timestamps during the validation period are identified as anomalies. We note that in both figures anomalies are most frequently observed for parts of the signal with a narrow uncertainty band. The cause of this behaviour has not been investigated, but we may speculate on a relation with deviations of the data from ideal the distribution function and/or data resolution.

$\alpha$	
----------	--

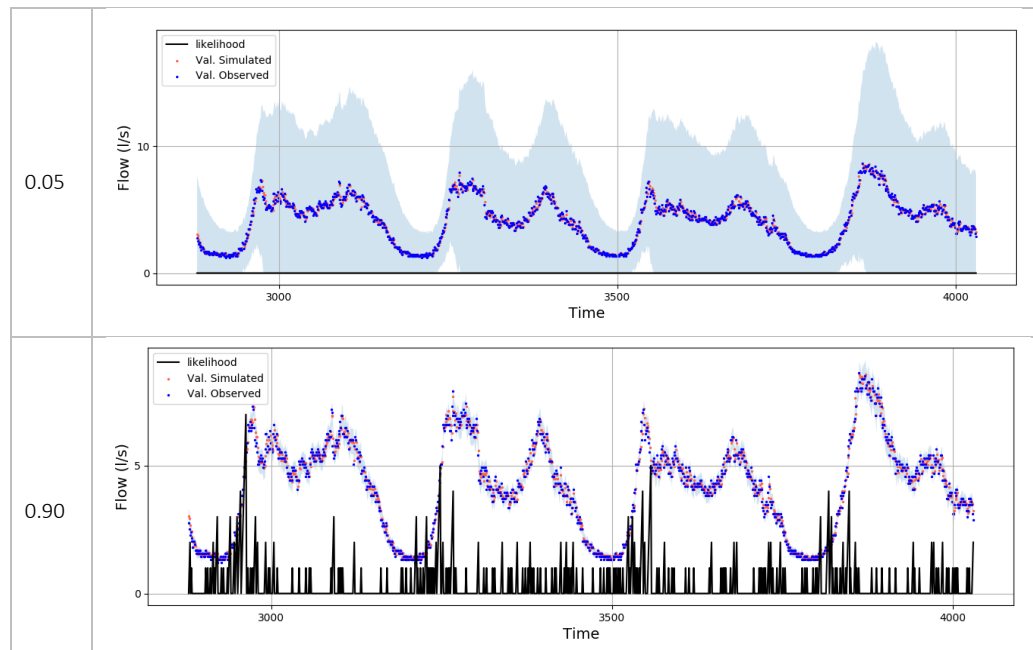


Figure 5. Sensitivity of anomaly detection of the autoregressive method as a function of the significance level  $\alpha$ . For values too small (in this case  $\alpha=0.05$ ), no anomalies are detected. For values too large (in this case  $\alpha=0.90$ ), an impractical number of meaningless anomalies is detected.

We note that to have an adequate amount of helps to get good results for this method. Though this also depends on location, season and time series resolution, as a rule of thumb we suggest 4 months of data. A possible refinement of the current implementation of the method is to perform separate analyses on weekend data and weekday data, or even on individual days of the week.

### 3.2.3 SPECTRAL ANALYSIS

This algorithm corresponds to the use of (as it names explicitly states) of spectral analysis or a Fourier transformation of the data into the frequency domain. A signal such as the one of consumption on a drinking water distribution network can be built based on the superposition of several harmonic (sinusoidal) functions. In the case of Callisto, this algorithm is elaborated following to the work developed by Eliades & Polycarpou (2012), in which the signal is decomposed in two steps.

Here we demonstrate the algorithm with an annual flow signal of a large city where two anomalies are introduced: (i) a leakage at the middle of June, and (ii) data which is removed from the time series during December (Figure 6 top). In fact the time series shows that daily operations register data of zero flows during a particular timestamp during the day. This anomaly was left in the signal.

In the first step of the algorithm, the signal is transformed into frequency domain and the long period (seasonal) components are removed (see Figure 6 bottom).

The remnant signal corresponds to the daily pattern and anomalies. Daily components are then also removed.

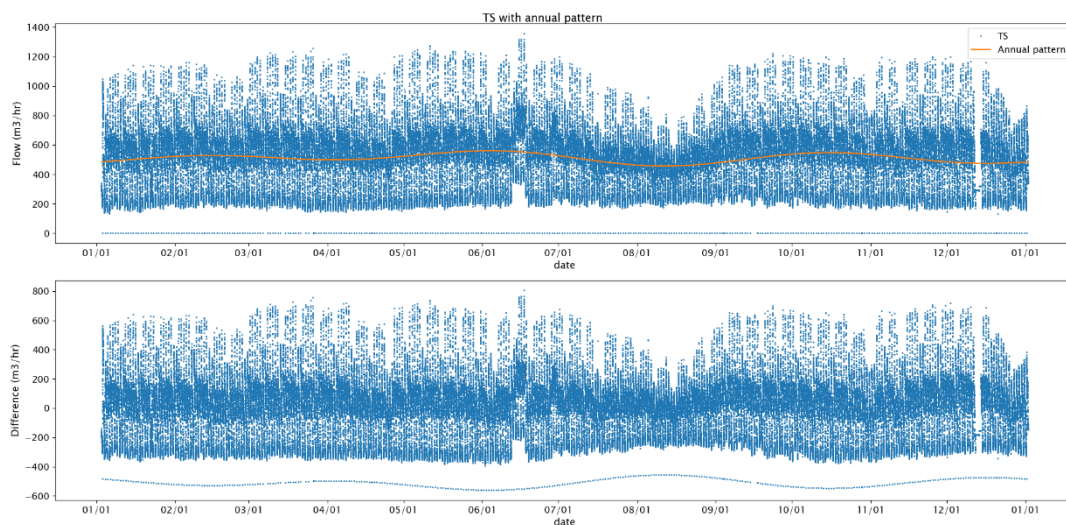


Figure 6. Annual pattern resulting from the spectral analysis.

In the second step, analysis of the residual signal is performed. What remains after this filtering of annual and daily patterns are the residuals (differences) of the signal. Next, the weekly pattern is extracted from the difference signal (Figure 7).

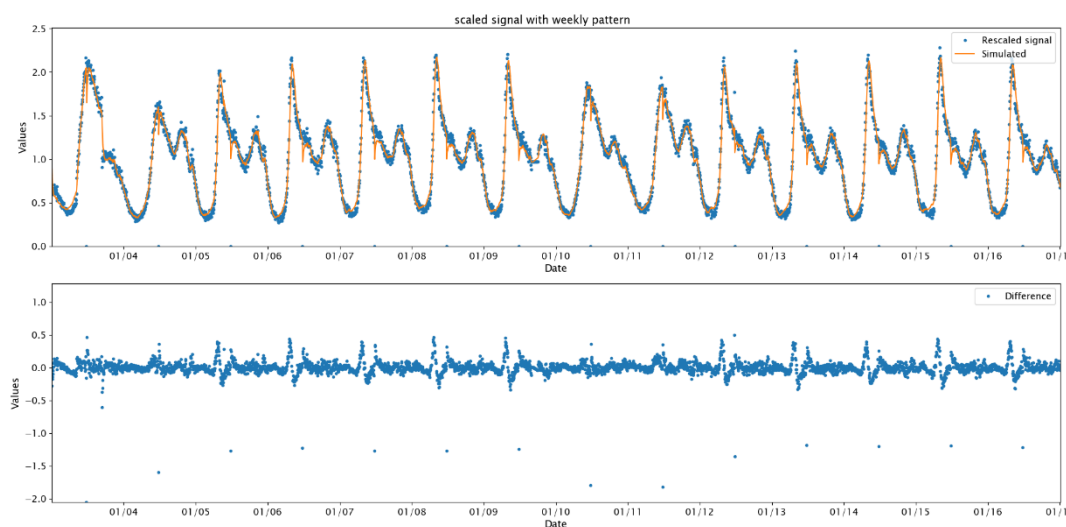


Figure 7. Top: weekly pattern obtained and the corresponding spectral reconstruction of the rescaled signal. Period corresponds to Jan 01-16. The bottom frame shows the difference between the signals, simulated and rescaled residual of annual) corresponds to the actual anomaly at each timestamp.

Finally, one proceeds to evaluate whether or not the residuals are significant, and therefore an anomaly can be identified or not (Figure 8). For this the algorithm uses a method from statistical quality control, the CUSUM (or cumulative sum control chart). This method corresponds to a sequential analysis technique typically used for monitoring change detection (Page, 1954). To determine when a change in the cumulative sum is considered significant, a single parameter is set within Callisto which defines the leakage size.

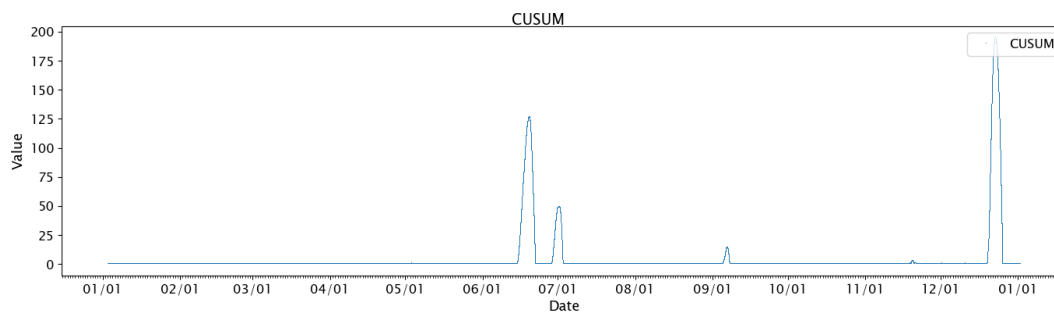


Figure 8. Spectral analysis anomaly detection using cusum. Notice that the two periods with largest cumulative sums correspond to the periods where the leakage has been added and where data was deleted from the time series.

### 3.2.4 SUPPORT VECTOR REGRESSION

Support Vector Regression is a machine learning algorithm of the supervised type. It is a method derivative of Support Vector Machines, a special type of neural network mainly used for classification purposes. In the case of Support Vector Regression a library of variables is built to forecast the behaviour of a signal (Vries, van den Akker, Vonk, de Jong, & van Summeren, 2016, Mounce, Mounce, & Boxall, 2011). In the case of Callisto, not only the data of the flows and pressures of measurements are used to construct the library of variables, but also some other variables such as day of the week (Monday to Sunday), hour of the day (0 to 23) are used for the prediction. Additional variables such as meteorological variables can be used, but this development is intended for operational forecast and falls outside of the boundaries of current application of Callisto. This algorithm has been broadly tested in the literature.

Support vector regression is controlled by a parameter  $\epsilon$ , which is the maximum error. This is the most critical parameter to take into account as it defines the threshold for the identification of a regression value of SVR as a possible leakage. Note that Support Vector Regression is a computationally intensive methods, requiring a significant computation time.

### 3.3 Leak Localization method

The leak localization method of Callisto couples an evolutionary optimization technique with heuristic network-traversal techniques to a pressure-driven hydraulic solver to accurately localize leakages. In essence it, it predicts flow and pressure (using a hydraulic model) at the locations of installed sensors for which data have been collected and tries to minimize the difference between observed and predicted flow/pressure by modifying hypothetical leakages in the hydraulic model, both their size and location. This is done in a structured way using an evolutionary optimization algorithm. Figure 9 give a concise overview of the algorithm.

The optimization algorithm OMNI Optimizer (Deb & Tiwari, 2008) has been previously applied in the context of leakage localization (Morley & Tricarico, 2016). The hydraulic engine (Morley & Tricarico, 2008) is an extension of EPANET 2.0 (Rossman, 2000). Leakages are located in nodes as emitters where the exponent has been fixed to 0.5, while the emitter coefficient ( $C_{Leak}$ ) can be varied depending on user needs.



Figure 9. Flowchart of the leak localization algorithm

### 3.4 Data Quality Control - Dataprofeet

Dataprofeet is a software tool developed by Witteveen+Bos Consulting Engineers with the purpose of performing anomaly detection on different data sources. The tool contains an extended set of data validation methods. Data

quality assessment can be customized for a specific data set by selecting the appropriate data validation methods and tuning the settings and critical values for each method.

Many validation tests are available but do not necessarily provide added value in determining the validity of a sample. Depending on the data set and signal types a well-thought combination of available validation tests is required to optimize the workflow and computation speed. For Callisto the following validation tests are considered to be sufficient to assess the quality of flow and pressure signals.

#### 3.4.1 Chronology

The leakage detection algorithms require the data to be in chronological order (newest samples last). If the data is not chronological the data will be sorted automatically. No user action is required.

#### 3.4.2 Missing

A regular interval between two consecutive samples is assumed. From the timestamps of the series the tool automatically determines the (regular) interval between two consecutive samples. Consecutive samples with a gap larger than the regular interval are detected. The tool adds the missing timestamp to the time series and marks it as missing. E.g. in case the dataset should contain a timestamp every half an hour, the regular interval is automatically set to 30 minutes.

#### 3.4.3 Bad / dead signal

Parts of the signal with too little variation is marked as a bad / dead signal. The method is applied with a moving time window. The length of the time window is fixated to be 1 day. If the standard deviation of the values of the series in a time window is below a given threshold, the complete window is marked as bad / dead signal. For Callisto this threshold is fixated at 0.1 units.

#### 3.4.4 Not A Number (NaN)

Non-numerical values in the dataset will be marked as NaN (Not a Number). In the case of pressure signals the value 0 is regarded as NaN.

#### 3.4.5 Linear trend

An automated test called "Seasonal Kendall" (Hirsch & Slack, 1984) is applied to input signals. This technique tracks down any potential congestion / drift in lines. This test requires a user specified value which represents the maximum allowed drift.

A description of this technique and its settings are as follows:

- The method is applied with a moving time window. If a linear trend is detected all values within the time window are marked. The method is applied to the time series as it is, hence there is no aggregation to e.g. hourly values.

Input parameters consist of:

- *Seasonality/periodicity of the signal*. A period of time after which the signal repeats itself. For Callisto the value is set to 1 day.
- *Significant slope*. Indicates the absolute threshold, i.e. the maximum allowed drift (in positive and negative direction) during a day. E.g. max allowance of 1 m<sup>3</sup> per day. If significant slope is 0, all statistically significant trends are marked and reported. This input variable is signal specific and can be used by the user to tune the strictness of the method. Default settings for pressure and flow signals is set to 0.
- *Window size*. The test can be performed on certain cuts (windows) of the time series. In Callisto the test is applied to a window length of 28 consecutive days. A shift can be given as an input such that windows overlap for more historical context. Choosing smaller window sizes might increase the accuracy of the method but the computational speed is significantly lowered.



As an example the time period April - May 2018 of flow signal Heemstede Totaal is depicted in Figure 10. A negative drift is evident from the picture. From April 13<sup>th</sup> onward the signal’s amplitude is decreasing up till the beginning of May.

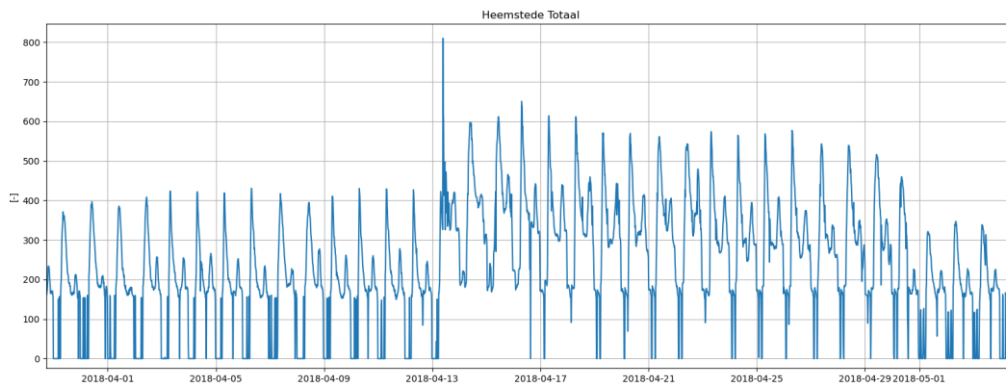


Figure 10. Heemstede totaal flow signal sample during April 2018.

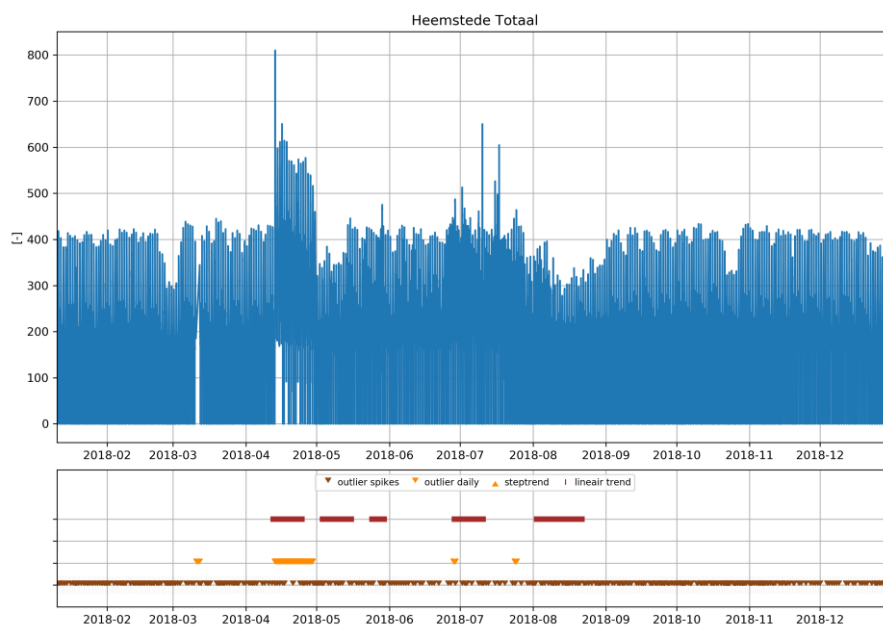


Figure 11. Linear trend result on Heemstede Totaal with significant slope: 1m<sup>3</sup> flow

The question arises whether the linear trend test marks this time period as drift. The linear trend results for test case Heemstede Totaal are shown in Figure 11. The default settings are used with user specific setting ‘Significant slope’ set to 1 m<sup>3</sup>. The negative drift from mid-April 2018 until May 2018 has been marked by the test.

### 3.4.6 Step trend

This validation test detects sudden jumps in a series. To be marked as a step trend the jump needs to be consistent for some time. A possibility for occurring step trends is dislocation of measuring devices.

A description of this technique and its settings are as follows:

- The method is applied to the time series as it is, hence there is no aggregation to e.g. hourly values.

Input parameters consist of:

- Number of samples which are tested at once. In Callisto the value is fixated to the amount of samples in a day. E.g. 96 samples (1 day if samples are registered every 15 minutes).
- Threshold. Maximum allowance for a jump. This threshold is automatically determined by the preprocessing tool. It calculates the allowance based on the variation in the signal. Signals with larger amplitudes are given a higher threshold.

The test cases of Heemstede and Diemen do not have any step trends. As an example a typical depiction of a step trend in a time series is included in Figure 12 **Error! Reference source not found.**

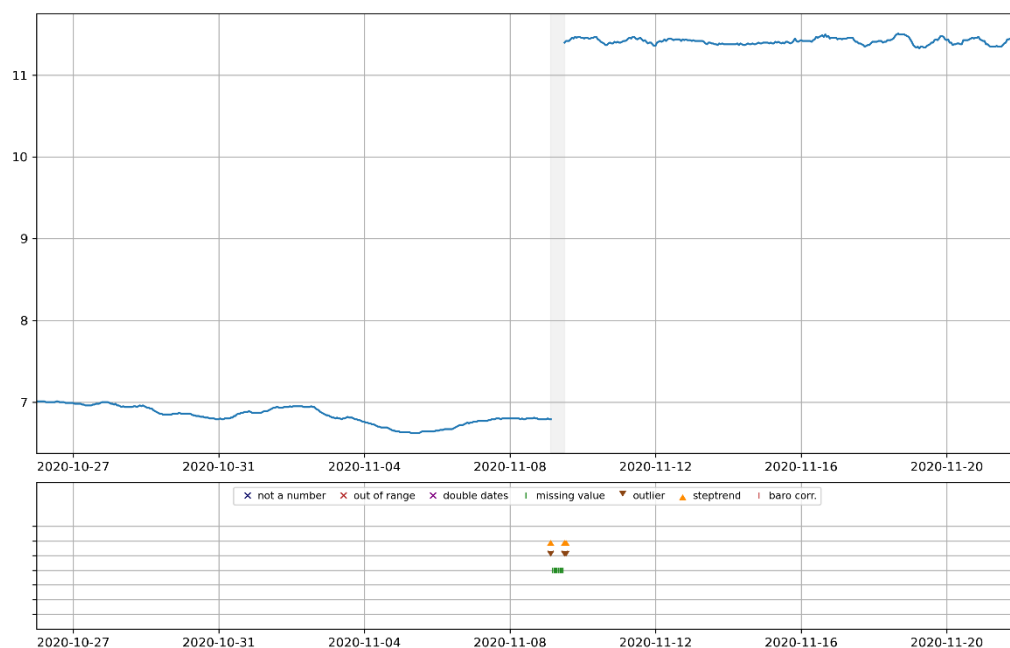


Figure 12. Example of a step trend in a time series

### 3.4.7 Double date

All timestamps should be unique. Identical timestamps will be marked. Identical timestamps with identical values are seen as duplicates. Duplicates (i.e. same timestamp and same value) are removed from the data set.

### 3.4.8 Interpolated

Sometimes the data contains linear elements which may be missing values that have been interpolated by the logger or sensor. These values are no accurate representation of the actual flow and will therefore be detected and marked as ‘likely interpolated value’.

### 3.4.9 Outlier Daily

This test uses the signal’s weekday patterns. Each weekday has its own pattern. As an example, this technique examines all Mondays at once by grouping them. Mondays which deviate too much from the average Monday pattern are marked as outliers in its entirety. A distinction is further made between night and day as each part of the day has a very distinctive pattern.

This outlier daily technique makes use of the following steps:

- The time series is cut in pieces and grouped by weekday (e.g. Monday) and day / night.

- The day / night distinction is required since small DMA's have erratic nights. The length of the day depends on the weekday.

This has been fixated as follows:

Day part: Monday to Saturday 07h-22h, Sunday 08h-22h

Night part: Sunday-Monday to Friday-Saturday 22h-07h, Saturday 22h-Sunday 08h

For each weekday and day/night:

- determine the median weekday (e.g. median Monday of all Mondays); the median Monday 9.15 pm value is the median of all available Monday 9.15 pm values;
- subtract median weekday from weekday values (e.g. subtract median Monday of timestamp 6.15 pm from all Monday's 6.15 pm);
- compute the mean absolute deviation (MAD) of the previous (subtracted) result;
- perform a statistical outlier test on the MAD's for the weekday;
- mark as an outlier if a particular day fails for the test.

Two examples of this validation technique have been depicted in Figure 13 and Figure 14. The former depicts the Tuesday patterns of the Heemstede flow signal. Red circles indicate failed test timestamps. The median of all Tuesdays is indicated by the red line. The figure depicts three dates (2018-04-17, 2018-04-24 and 2018-07-24) for which the daily pattern (strongly) deviates from the median line. The part of the day that failed the test (in this case day and night) are marked in their entirety as 'Outlier daily'. In the case of Figure 14 the Wednesday patterns of Heemstede's pressure signal is pictured. For failed date 2018-01-10 only the night part deviates excessively from the median. Hence only the night part is marked. As for date 2018-05-02 the whole water consumption is constantly (significantly) lower than the median line. Note that marking like this may signal a data quality issue, but also a leak event. It is up to the user, with the help of the leak detection methods implemented in the tool, to make the distinction.

#### 3.4.10 Outlier Spike

Sudden peaks in the signal are marked with this test. The test is only applied to the day part. For small DMA's night signals tend to become irregular and erratic, resulting in a lot of false positive spikes.

This technique follows the following steps:

- The series is cut in pieces and grouped by weekday (e.g. Monday) and day / night.
- The night part will not be tested since the night consists of many spikes, giving rise to a lot of outlier spikes flags.
- All dates which are on the same weekday (e.g. Monday) will be placed together, resulting in a new series.
- For each weekday the median weekday series is determined.
- The difference is calculated between tested Mondays and the median Monday.
- The 'normal' Dataprofeet outlier test will be performed on this 'difference series'.

Input parameters consist of:

- Number of samples which are tested at once; i.e. the window. In Callisto the window is fixated to 5 samples. Using more samples for the window is not advisable as the chance of more spikes being present in the window increases. In that case the tool will detect these spikes as being normal to the data set, resulting in not being marked as an outlier. Threshold. Maximum allowance for a jump. This threshold is automatically determined by the preprocessing tool. It calculates the allowance based on the variation in the signal. Signals with larger amplitudes are given a higher threshold.

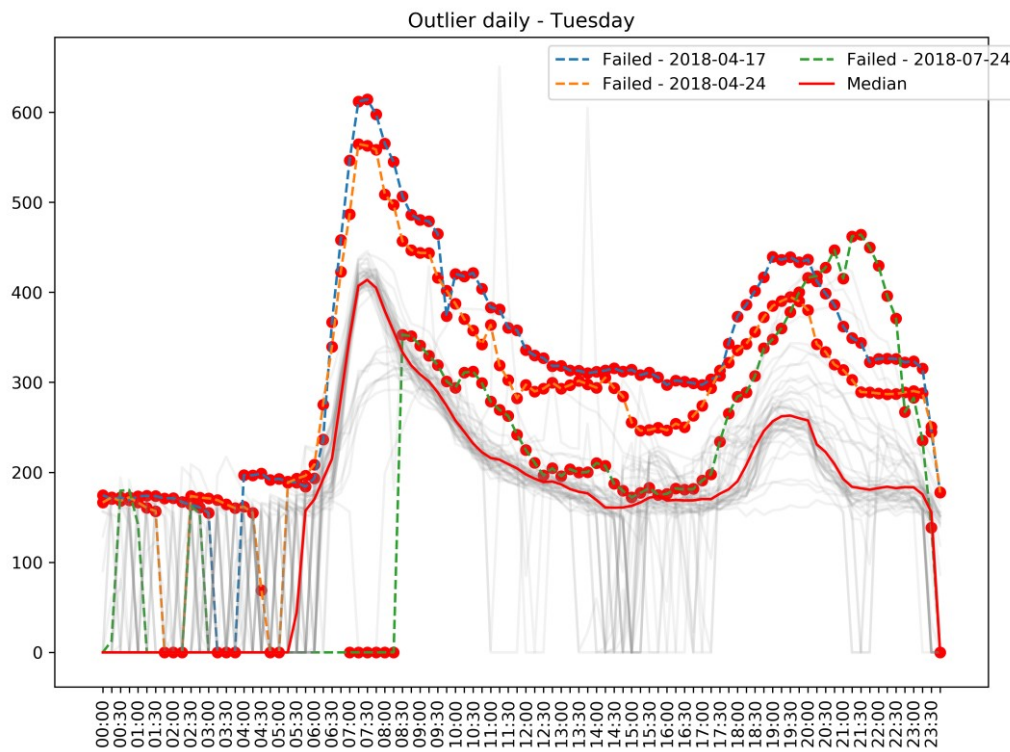


Figure 13: Outlier daily - Heemstede flow signal. Daily patterns for day of the week: Tuesday.

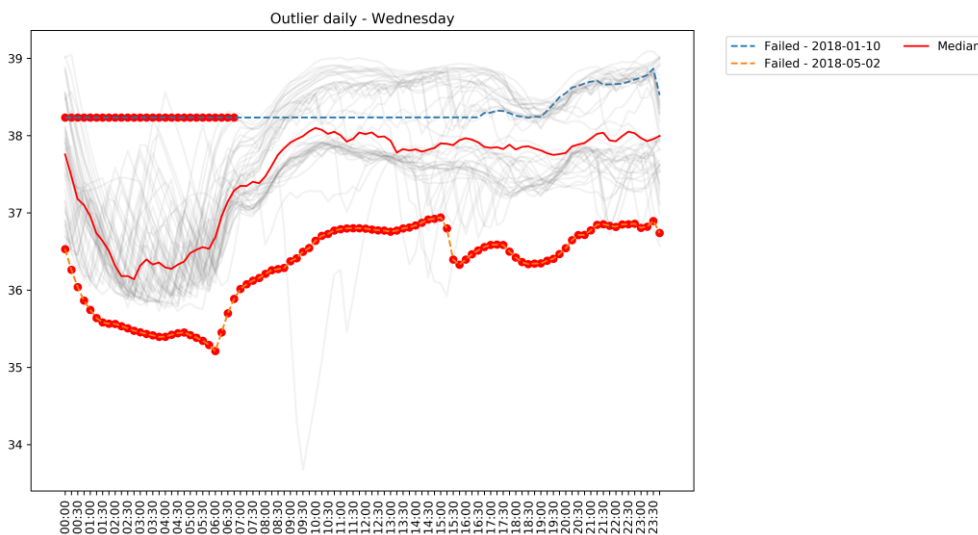


Figure 14. Outlier daily - Heemstede pressure signal. Daily patterns for day of the week: Wednesday.

In Figure 15 and Figure 16 the results are shown of the outlier spike test. As the weekday data is compared to the weekday median line not all 'spikes' have to be marked. This is the case when both the median and the tested weekday have the same magnitude spike.

Only the timestamps which the outlier spike test has indicated as being spikes will be marked.

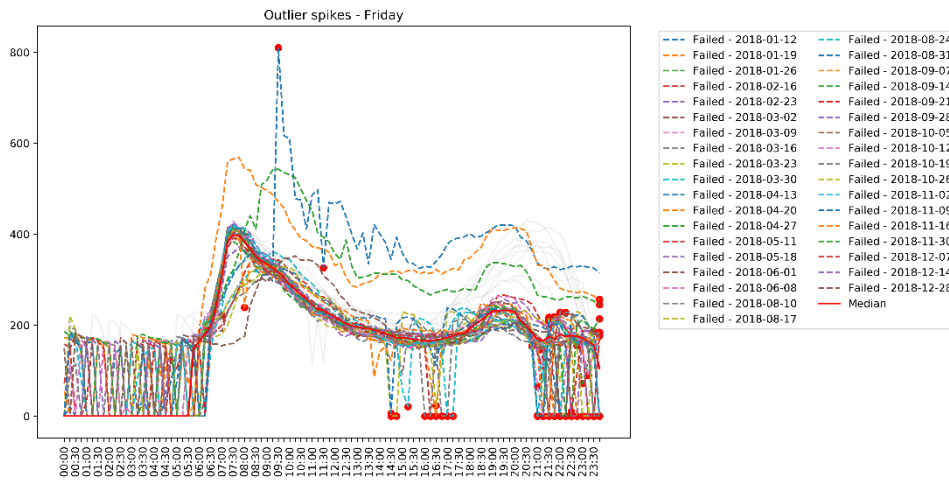


Figure 15. Outlier spike - Heemstede flow signal. Daily patterns for day of the week: Friday.

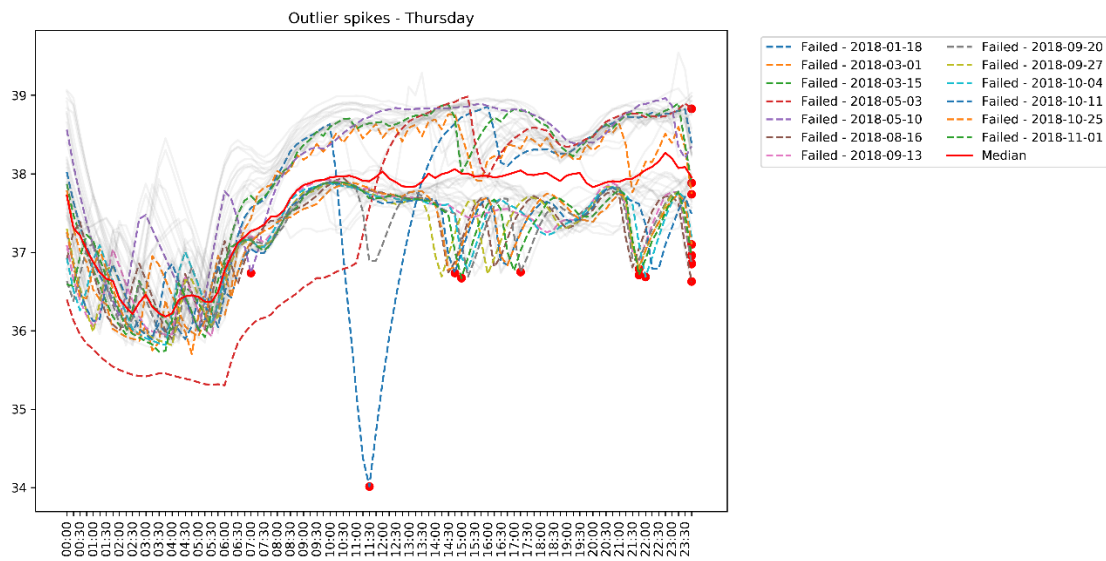


Figure 16. Outlier spike - Heemstede pressure signal. Daily patterns for day of the week: Thursday.

## 4 Callisto tool

Based on the choices described in the previous chapter, the Callisto tool was developed. An impression of the tools main screen is provided in Figure 17.

The tool consists of:

- functionality for importing and editing raw signals;
- a Signal Explorer that gives the user direct visual access to all time series, including raw and processed data and analysis results;
- a pre-processing module that allows the user to identify and fix data quality issues;
- four leak detection modules;
- functionality for importing hydraulic models for the purpose of leak localization;
- a leak localization module.

The user can choose to apply one or multiple leak detection modules and interpret the results individually or in a combined manner. Note that the tool has been built in such a way that additional leakage detection and/or localization methods can be added relatively easily. For a complete description of the Callisto tool, the reader is referred to the Callisto user manual (Quintiliani and Castro Gama, 2020).

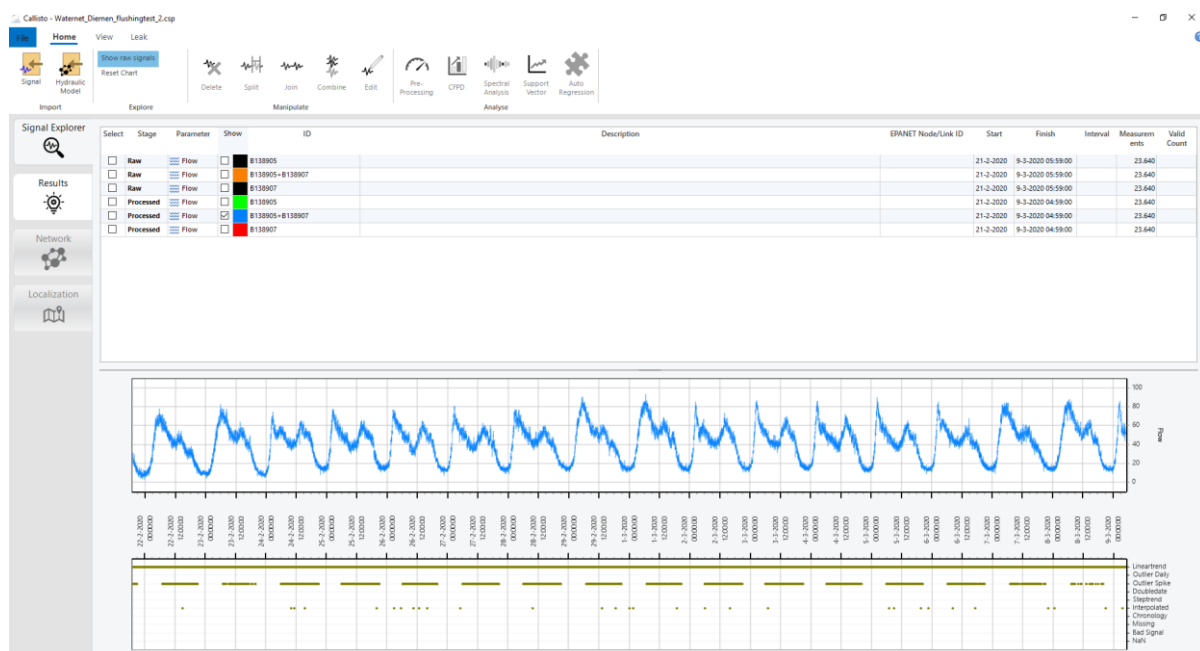


Figure 17: The main screen of the Callisto tool.

# 5 Case studies

## 5.1 Selection of case studies

In order to test the Callisto tool on real data with known leakages, two case studies were proposed, in which leakages were simulated by flushing from a hydrant. One case study site was offered by Waternet (Diemen-Noord) and one by Dunea (Duindorp), see Table 5. For each of them the information of DWDN models and historical records were collected. Other different datasets available by KWR of different DWDN were available in order to perform debugging and characterization of the leak detection methods.

Table 5: Some characteristics of the case study areas.

Case study	number of connections	number of consumers	pipe length
Duindorp	2234	6000	12.9 km
Diemen-Noord	2853	7304	17.4 km

## 5.2 Historical records

In the case of Diemen-Noord data of 2015 was supplied for the whole year. Data is available at a resolution of 15 min. In Figure 18, the time series for the two incoming pipes is presented. The total incoming flow corresponds to the bottom subfigure.

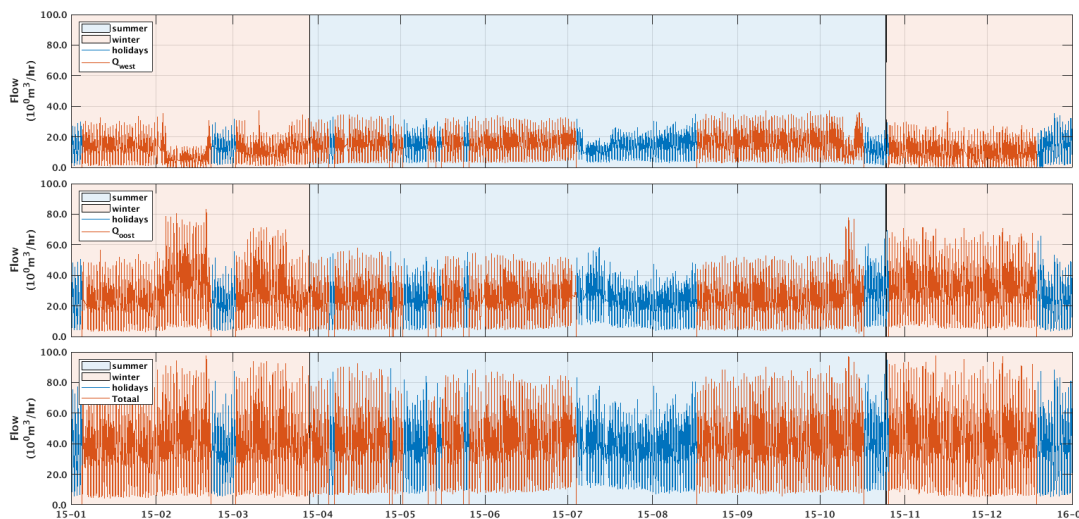


Figure 18. Time series of flows at the inlet (west & oost) of Diemen-Noord operated by Waternet. The different seasons, winter and summer, are presented (daylight savings time period in light blue). In addition some holiday weeks are highlighted (in blue) to demonstrate how variable the consumption is in this location.

Data from Duindorp was available in the period of January 2017 until April 2019. The time series is presented in Figure 19.

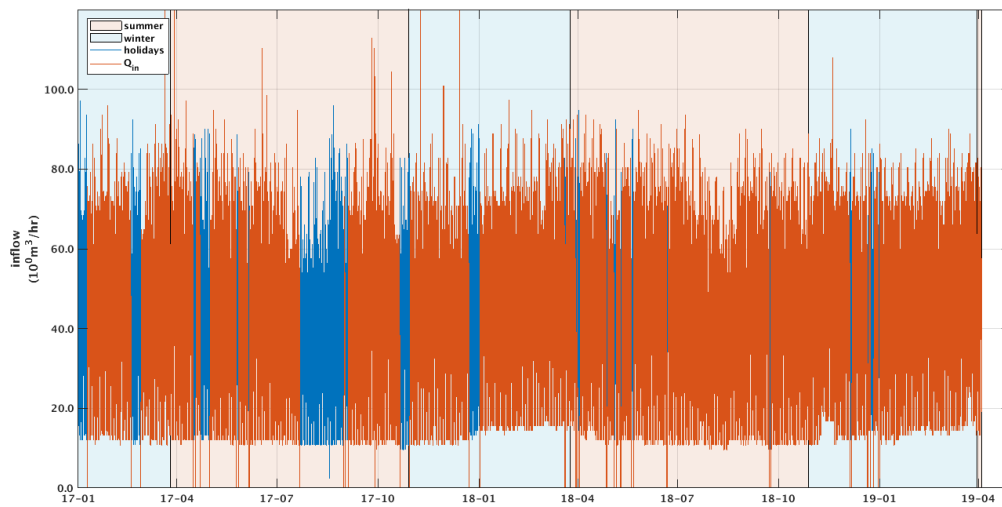


Figure 19. Time series of flows at the inlet of Duindorp operated by Dunea. The different seasons, winter and summer, are presented (daylight savings time period in light blue). In addition some holiday weeks are highlighted (in blue) to demonstrate how variable the consumption is in this location.

### 5.3 Flushing tests

With the goal of testing both the leak detection and the leak localization algorithms a proposal was made to the utilities to perform flushing tests to simulate leakages. A handout (see Appendix) was delivered with a proposal of locations where the flushing tests could be of interest based on the hydraulic model.

After the flushing tests were performed the locations of the flushing tests were kept secret to KWR and Witteveen+Bos by both utilities. The purpose was to have blind sample of tests for the testing of the localization algorithm.

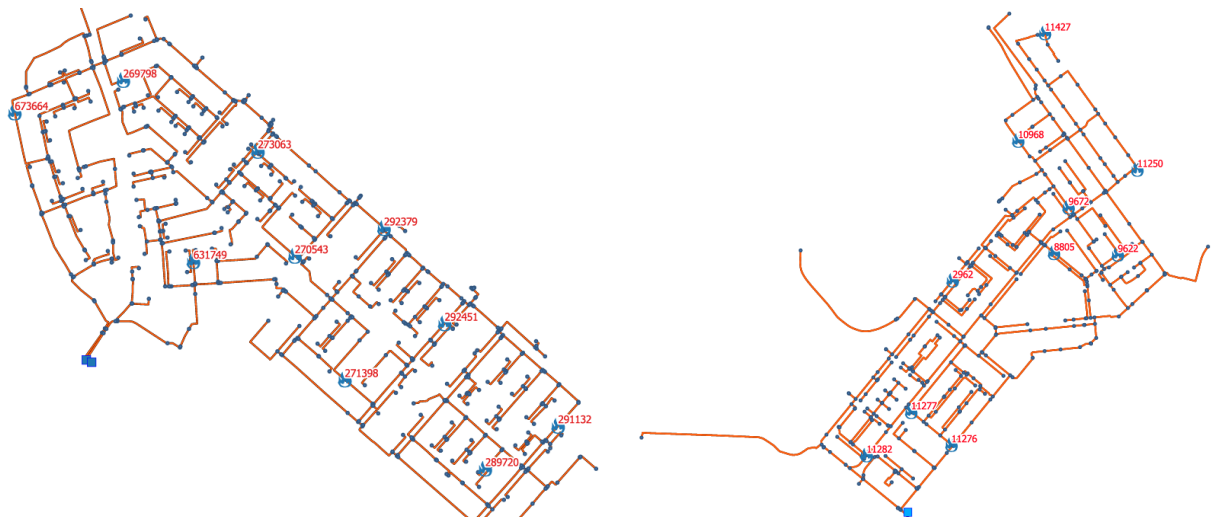


Figure 20. Proposed locations of flushing tests for Diemen-Noord (left) and Duindorp (right).

### 5.4 Data of time series of flushing tests.

After performing the flushing tests both utilities returned the corresponding time series of the two case studies. For Duindorp a total of 7 time series were obtained as presented in Table 6. For the purposes of the application of the data within Callisto the time series were interpolated to maintain the same timestamps throughout.



Table 6. Time series data obtained from dunea for duindorp. The flushing tests are short events within the longer time series.

<i>id</i>	<i>Name</i>	<i>Variable</i>	<i>Initial date</i>	<i>final date</i>	<i>dt (min)</i>
1	Bruinbankstraat	Pressure	01-01-20 00:01:00	13-04-20 23:59:00	1
2	Doggersbankstraat	Pressure	01-01-20 00:01:00	13-04-20 23:59:00	1
3	Schiermonnikoogsestraat	Pressure	01-01-20 00:01:00	13-04-20 23:58:00	2
4	Terschellingsestraat	Pressure	01-01-20 00:01:00	13-04-20 23:58:00	2
5	Walchersestraat	Pressure	01-01-20 00:01:00	13-04-20 23:55:00	5
6	Duivelandsestraat P	Pressure	01-01-20 00:01:00	13-04-20 23:55:00	5
7	Duivelandsestraat F	Flow	01-01-20 00:01:00	13-04-20 23:55:00	5

For the case of Diemen-Noord the two inflow signals were delivered corresponding to data of 2020 between February 4 and March 9 (Table 7).

Table 7. Time series data obtained from Waternet for Diemen-Noord. The flushing tests are short events within the longer time series.

<i>TS</i>	<i>Name</i>	<i>Variable</i>	<i>initial date</i>	<i>final date</i>	<i>dt (min)</i>
8	Oostleiding	Flow	04-02-20 00:00:00	09-03-20 09:59:00	1
9	Westleiding	Flow	04-02-20 00:00:00	09-03-20 09:59:00	1

### Hydraulic models used for leak localization

In addition, hydraulic models for the two case study areas were supplied by their respective water utilities. Table 8 presents their main characteristics; Figure 20 shows their topology.

Table 8. Summary of main characteristics of the hydraulic models for the two case studies.

<i>Item</i>	<i>Duindorp (Dunea)</i>	<i>Diemen-Noord (Waternet)</i>
Number of Junctions	430	838
Number of Reservoirs	1	2
Number of Tanks	0	0
Number of Pipes	452	605
Number of Pumps	0	0
Number of Valves	0	247

## 5.5 Execution of flushing tests

Figure 21 gives an impression of the setup and execution of a flushing test.

a)



b)



c)



d)



Figure 21: Setup of a flushing experiment by Waternet.

## 6 Results

### 6.1 Introduction

This chapter provides an overview of both synthetic tests and analyses that illustrate the correct functioning and demonstrate the performance of the tool and the results of the analyses performed on the data acquired in the flushing tests in both case study areas, with a comparison to the actual flushing event data. It must be noted that the analyses of the field data (sections 6.3 and 6.4) are somewhat rudimentary, performed under time constraints and with a developing understanding of the methods and tool. The analyses performed on synthetic data (sections 6.2 and 6.5) have been more rigorous.

### 6.2 Method and sensitivity testing on synthetic data

Before analysing the collected data, an extensive series of tests and sensitivity analyses was performed. The hydraulic model of Diemen-Noord was used to predict flow and pressure time series corresponding to a large number of synthetically generated leaks in the model (see Box 1). Varying levels of noise were applied to these time series before performing a leak detection and localization analysis on them using the Callisto tool. An overview of the localization results is presented in Figure 22. This figure shows the distance of the best leak localization result compared to the actual leak location for varying noise levels in the signal (0-4%) and varying leak magnitudes. As leakage magnitudes are pressure dependent, and simulated as such, the reported numbers do not directly represent flow rates, but rather leakage coefficients. The results presented in the figure demonstrate that for noise levels up to 4%, leakages can often be located within 100 meters, and almost always within 200 meters, for all leakage magnitudes studied. For higher noise levels, the performance is expected to deteriorate. It would be very interesting to determine at which noise level the localization becomes unreliable. It is highly recommended to include this aspect in any possible follow-up work.

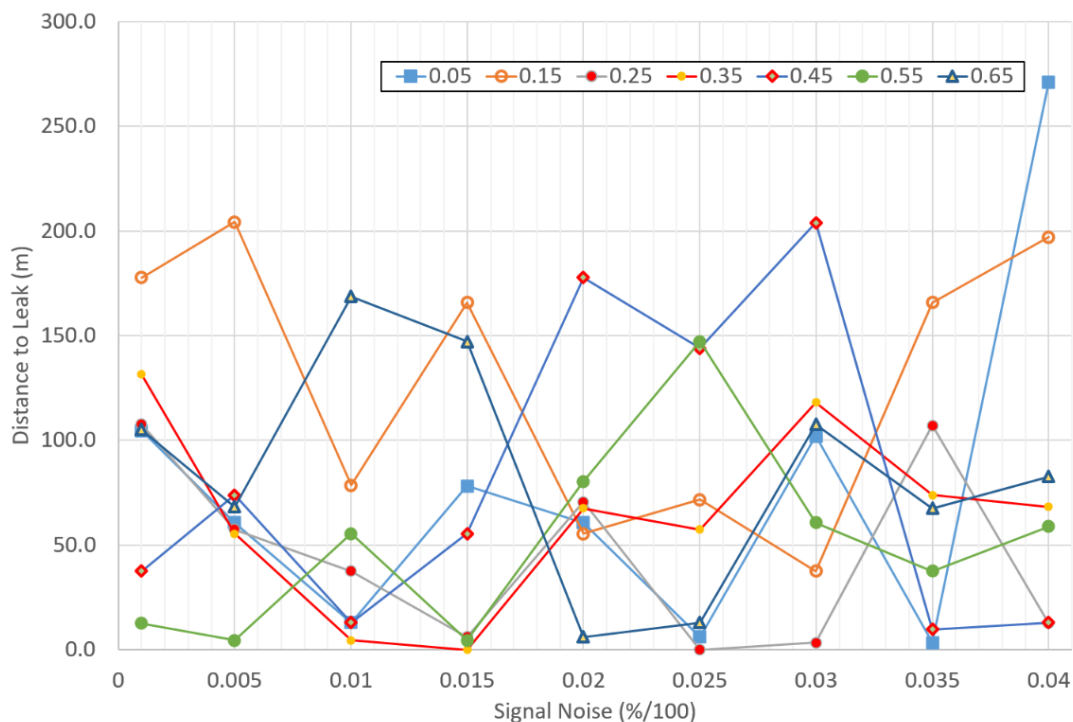


Figure 22: Overview of sensitivity testing results on the Diemen-Noord model. Different colours represent different leakage coefficient values.

**Box 1: Simulating leakage**

In the hydraulic model used, a leak can be simulated by adding an additional pressure dependent demand to a node. The following formulation is used;

$$Q = C * p^{0.5}$$

in which Q is the flow, C the leakage coefficient, and P the local (undisturbed) pressure.

For example, if the local undisturbed pressure at a node is 31 meters, and a leak has a known flow rate of 4 m<sup>3</sup>/h, this leak would be simulated by applying a leakage coefficient  $C=4/31^{0.5}=0.72$ .

**6.3 Flushing experiments - Duindorp**

**6.3.1 Leak detection**

Callisto has been applied to the data of Dunea for this location. All four leak detection methods, i.e. CFPD, Spectral analysis, Support Vector Regression and Autoregressive analysis were applied to the time series.

- The results of CFPD applied to the flow data show that during week 13 changes occurred at this location (see Figure 23).
- The Spectral Analysis also shows that an anomaly in the volume signals can be identified (see Figure 24).
- SVR also reveals that an anomaly must have occurred in this location during the same time window (see Figure 25).
- Finally the application of autoregressive (Figure 26) confirms also that there is anomaly in the signal during week 13, however the largest anomaly in the case of this detection method occurs during week 3.

The combined results give confidence that a relevant event occurred in week 13 and possibly also in week 3. An additional anomaly is detected by both SVR and AR on March 6.

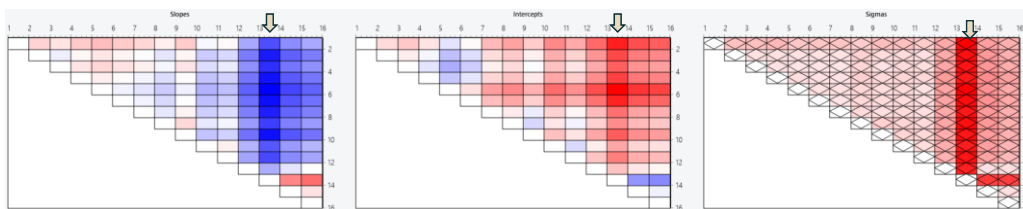


Figure 23. Results of CFPD on volume at inlet in Duindorp. There is a visible change in slope (left) and intercept (middle) during week 13. This highlights the possibility of a leakage. The fact that the standard deviation (right) is also quite high in this week indicated that the event lasted for a period of time shorter than a week.

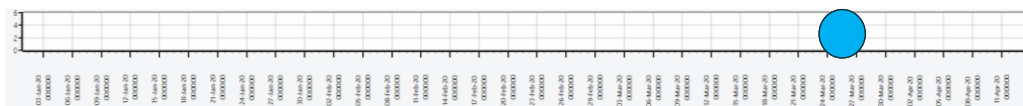


Figure 24. Results of spectral analysis on volume at inlet in Duindorp. There is a clearly visible signal week 13, this highlights the possibility of a leakage.

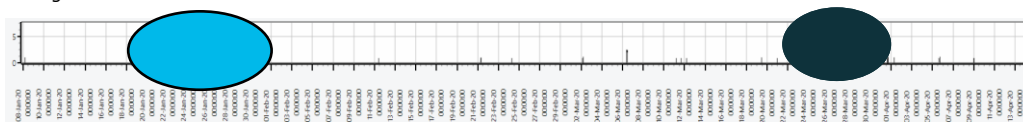


Figure 25. Results of SVR analysis on volume at inlet in Duindorp. The same anomaly can be identified as in Figure 23 and Figure 24. Noteworthy are one high likelihood and several smaller likelihood detections in week 13, and also a number of smaller likelihood detections in week 3.

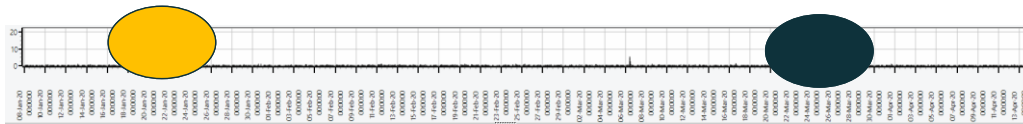


Figure 26. Results of autoregressive analysis on volume at inlet in Duindorp.

### 6.3.2 Leak Localization

Given that there is a consistent identification of one or more anomalies during week 13, the localization was performed constraining the leakage emitter coefficient between 0.01 and 5.0 (these numbers can be constrained using the magnitude and the time window for the occurrence of the flushing test between day 3 and day 15 of the model simulation. The duration was constrained between 1 and 48 hours. The analysis with these constraints results in a population of 200 possible solutions of which seven locations are feasible. From this list of leak locations those with the smallest error are presented in Table 9 and shown on a map in Figure 27. Leak localization obtained for week 13 at Duindorp. Location at Duivelandsestraat. Figure 27.

Table 9. Results of Callisto’s localization in Duindorp.

Rank	ID node	Frequency
1	K4357349DEH	83
2	L120248147DEH	71
3	B4357331DEH	16
4	L120248191DEH	15

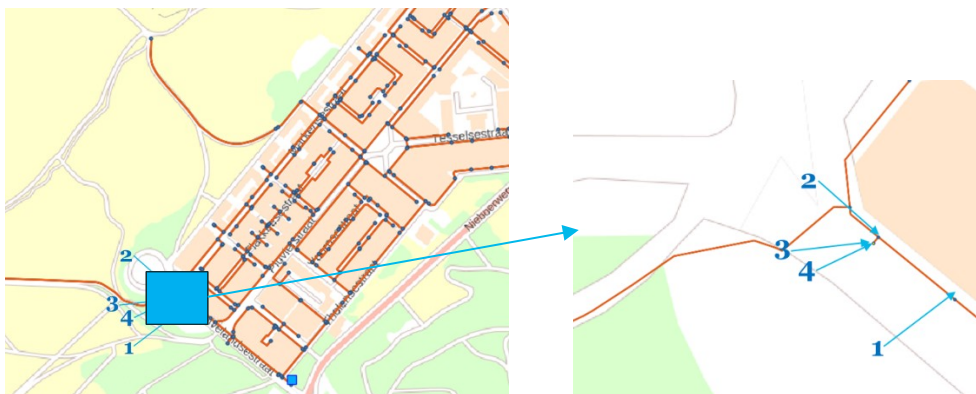


Figure 27. Leak localization obtained for week 13 at Duindorp. Location at Duivelandsestraat.

According to the localization algorithm the date of occurrence is 24 March 2020, the algorithm also estimates that the simulated leakage must have initiated between 08:35 and 09:05, with a total duration of approximately 12 hours. Such information was corroborated with the utility who have declared this result is incorrect. Then the reasons for the erroneous localization of the leakage in this DMA were investigated.

### 6.3.3 True characteristics of flushes and failure analysis

The true locations and timings of the flushing experiments are presented in Table 10. They are plotted and compared to the anomalies which were detected in the analysis of section 6.3.1 in Figure 28. Note that the incompletely registered event ending on March 29 has not been included. We note that three small flushing tests have not been detected. The week in which the large 100 m<sup>3</sup>/h flushing test was performed has been flagged as anomalous.

Table 10. True location of flushing tests to simulate leakages at Duindorp

Flushing	Adres	Epenet ID ??	Bk nummer	Start		Eind		Debiet	Diameter	Material
1	Zeezwaluwstraat 281	B1125717DEH = true	10968	12-Mar-20	10:00	13-Mar-20	08:00	4 m3/uur	110	PVC
2	Houtrustweg/gruttostraat 1	K350840748DEH = true	-	25-Mar-20	09:50	25-Mar-20	11:00	100 m3/uur	150	NGIJ
3*	Zeezwaluwstraat 261	K1125624DEH = true	-	??	??	29-03-20	??	??	28	cu
4	Zeezwaluwstraat 47	K278714285DEH = true	9621	30-mrt-20	12:30	31-mrt-20	13:30	4 m3/uur	110	PVC
5	Meeuwen 11	B240961613DEH = true	9622	8-apr-20	10:15	9-apr-20	08:30	4 m3/uur	110	PVC

\* Action/Leak 3 is dismissed as we do not know anything about it

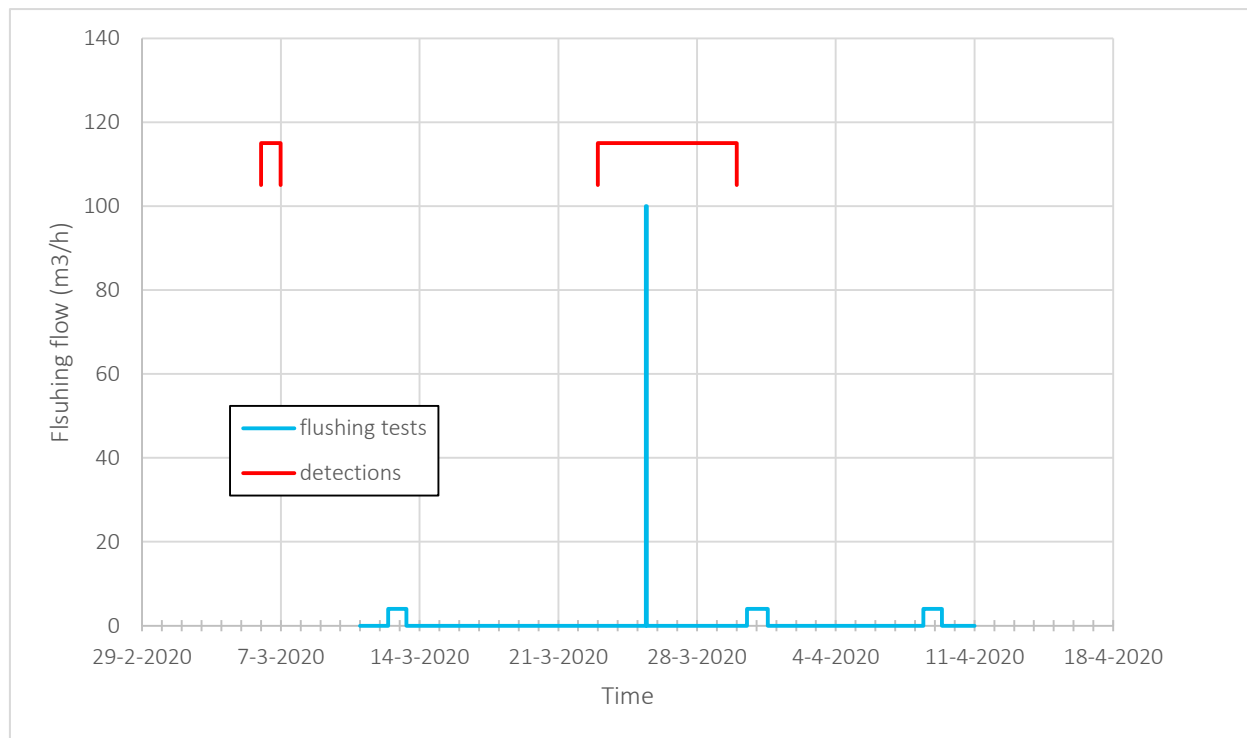


Figure 28: Comparison of simulated leaks and detected anomalies for Duindorp.

A number of factors can be indicated that offer possible (partial) explanations of the failure to correctly locate any flushing event, even though the second has such a magnitude that it can hardly be missed:

- The leakage detection was performed at the level of weekly data, but no zoom-in on a shorter time scale was performed using the CFPD analysis. Also, no magnitude was determined in the leak detection phase. This resulted in inadequate constraints for the leak localization.
- Confidence in the hydraulic model that is applied needs to be established before starting the analysis. The model provided turned out to contain a significant underestimation of the actual demand, which is critical for the performance and representativeness of the hydraulic simulations. Also, the location of an inflow sensor was incorrect (Figure 29). An additional point of concern is the use of a single demand pattern for all demand nodes, which is not representative of the stochastic nature of real demand. In the framework of this project, it has not been ascertained to what degree this influences the capacity of the leak localization algorithms to localize leakages in real world networks.

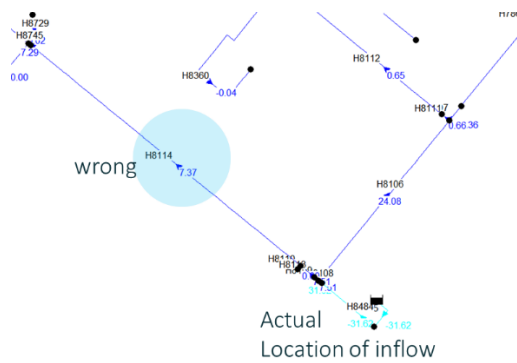


Figure 29. Actual location of inflow sensor in Duindorp.

## 6.4 Flushing experiments in Diemen-Noord

### 6.4.1 Leak detection

Callisto has been applied to the data of Waternet for this location. All four leak detection methods, i.e. CFPD, Spectral analysis, Support Vector Regression and Autoregressive analysis were applied to the time series. The day numbering used in the analysis is shown in Table 11.

- The CFPD analysis shows a clear period of anomalies (positive inconsistent change, meaning increased constant demand) from day 22 to day 34, i.e. the 25<sup>th</sup> of February until the 8<sup>th</sup> of March, and a less clear one on days 15-18, i.e. 18 to 21 February, see Figure 30.
- Spectral analysis (Figure 31) shows a number of short anomalies (positive demand peaks) between February 29 and March 9, see Table 12.
- The autoregressive analysis (Figure 32) identifies potential anomalies on February 25, 27, and March 2, 7, and 8. The most likely anomalies are on February 25, and March 7 and 8.
- No successful analyses using Support Vector Regression was completed for this dataset.

Many anomalies were detected by at two methods (although the CFPD analysis shows a complete anomalous period, also identified by spectral analysis). Two anomalies, on March 7 and 8, are seen by three methods. Table 13 provides an overview.

Table 11: Day numbering of the Diemen-Noord flushing experiment data.

Day No	Week No	Date	Weekday	Name
1	1	2020-02-04	2	Tuesday
2	1	2020-02-05	3	Wednesday
3	1	2020-02-06	4	Thursday
4	1	2020-02-07	5	Friday
5	1	2020-02-08	6	Saturday
6	1	2020-02-09	7	Sunday
7	2	2020-02-10	1	Monday
8	2	2020-02-11	2	Tuesday
9	2	2020-02-12	3	Wednesday
10	2	2020-02-13	4	Thursday
11	2	2020-02-14	5	Friday
12	2	2020-02-15	6	Saturday
13	3	2020-02-16	7	Sunday
14	3	2020-02-17	1	Monday
15	3	2020-02-18	2	Tuesday
16	3	2020-02-19	3	Wednesday
17	3	2020-02-20	4	Thursday
18	3	2020-02-21	5	Friday
19	4	2020-02-22	6	Saturday
20	4	2020-02-23	7	Sunday
21	4	2020-02-24	1	Monday

22	4	2020-02-25	2	Tuesday
23	4	2020-02-26	3	Wednesday
24	4	2020-02-27	4	Thursday
25	5	2020-02-28	5	Friday
26	5	2020-02-29	6	Saturday
27	5	2020-03-01	7	Sunday
28	5	2020-03-02	1	Monday
29	5	2020-03-03	2	Tuesday
30	5	2020-03-04	3	Wednesday
31	6	2020-03-05	4	Thursday
32	6	2020-03-06	5	Friday
33	6	2020-03-07	6	Saturday
34	6	2020-03-08	7	Sunday
35	6	2020-03-09	1	Monday

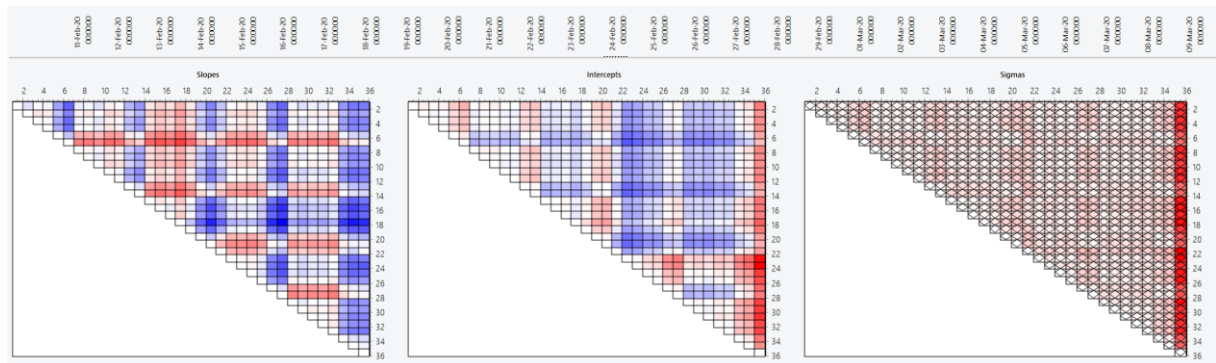


Figure 30: CFPD analysis results for the Diemen-Noord flushing experiments.





d)

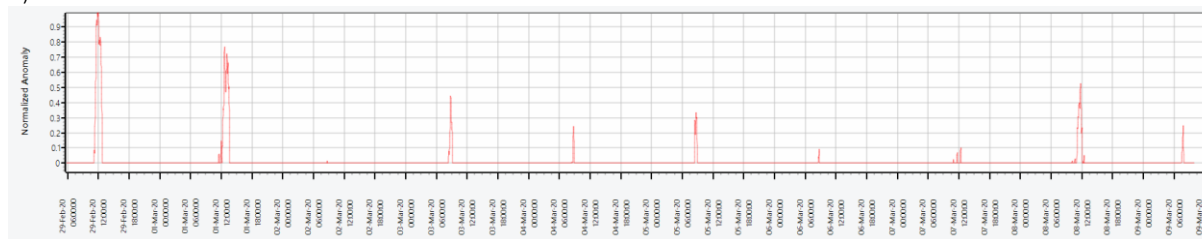


Figure 31: Overview of spectral analysis results for Diemen-Noord. a) SA for leak magnitude of 4.0 m<sup>3</sup>/h. b) SA for leak magnitude of 1.0 m<sup>3</sup>/h. c) and d) SA for a leak magnitude of 2.0 m<sup>3</sup>/h.

Table 12: Anomalies detected by the spectral analysis for Diemen-Noord.

Id	Date	Anomaly (peak)	Start time	End time
1	Feb 29	1.00	11.00	12.45
2	Mar 01	0.75	12.00	13.40
3	Mar 03	0.45	08.00	09.10
4	Mar 04	0.25	08.30	09.00
5	Mar 05	0.32	08.00	08.55
6	Mar 06	<0.1	08.30	08.47
7	Mar 07	<0.1	3 pulses, first at 10.30	3 pulses, last at 12.30
8	Mar 08	0.5	11.00	12.10
9	Mar 09	0.25	07.00	08.00

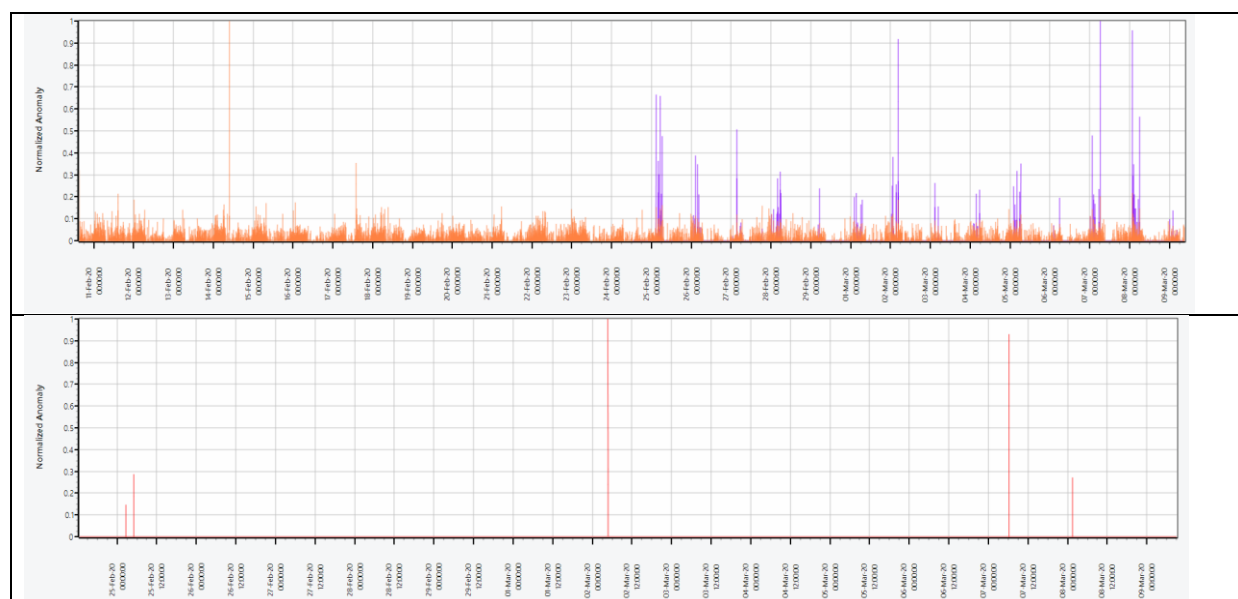


Figure 32: Leak detection results for the autoregressive method. a) For two sets of settings (orange: small training set,  $\alpha_{ci}=0.85$ ; purple: large training set,  $\alpha_{ci}=0.50$ .) b) For an additional analysis with a large training set and  $\alpha_{ci}=0.15$ .

Table 13: Combined leak detection results for Diemen-Noord. The most likely candidates are March 7 and 8.

Date	Spectral analysis			Autoregressive	CFPD	method count
	Anomaly (peak)	Start time	End time			
Feb 25				likely	x	2
Feb 27				possible	x	2
Feb 29	1.00	11.00	12.45		x	2

	Spectral analysis			Autoregressive	CFPD	method count
Date	Anomaly (peak)	Start time	End time			
Mar 01	0.75	12.00	13.40		x	2
Mar 02				possible	x	2
Mar 03	0.45	08.00	09.10		x	2
Mar 04	0.25	08.30	09.00		x	2
Mar 05	0.32	08.00	08.55		x	2
Mar 06	<0.1	08.30	08.47		x	2
Mar 07	<0.1	3 pulses, first at 10.30	3 pulses, last at 12.30	likely	x	3
Mar 08	0.5	11.00	12.10	likely	x	3
Mar 09	0.25	07.00	08.00			2

#### 6.4.2 Leak localization

Leak localization was performed using the Callisto tool to isolate a single leakage the period of February 24 to March 1. Based on the analysis presented above, it is likely that multiple flushing events took place during this period, so multiple solutions may be valid. The list of most likely locations are presented in Table 14 including the number of times each node appears as a solution (frequency). All solutions show a leakage on February 29.

*Table 14: Most likely nodes for the flushing tests in Diemen-Noord. Note that multiple events may be represented in these results and therefore multiple nodes may be valid. The reported frequency can be considered a measure for the likelihood.*

Node id	frequency	Node id	frequency	Node id	frequency
No41	56	A044990	4	A044987	2
A044071	55	No188	4	No284	2
A044069	25	A044064	3	A044063	1
A044070	13	No120	3	No117	1
No187	10	No185	3	No186	1
A048545	7	No42	3		
A044065	5	A044068	2		

The estimated durations range between 7 hours and 8 hours for half of the solutions. Note that the root mean square error of the flow is 11.56 m<sup>3</sup>/h, which is about 1/3 of the mean flow. This indicated that there is a significant difference between the hydraulic model and the real situation in the field - this model appear to be too diverged from reality to be effective with Callisto. This is also illustrated by the fact that the hydraulic model has a midnight flow of approximately 10m<sup>3</sup>/h, whereas the observed data starts off at 27m<sup>3</sup>/h. Real peak hour consumption, on the other hand, peaks at roughly the same values as the model.

The location of the first nodes of the list is presented in Figure 33. We do not consider it likely that this is the actual location.

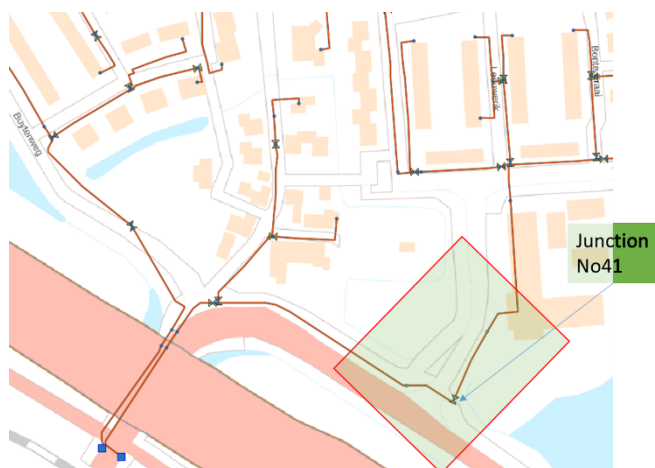


Figure 33: Reconstructed location for one of the flushing tests. Note that it is likely to be wrong because of the large difference in flow between model and observations.

### 6.4.3 True characteristics of flushes and analysis

An overview of the true locations, timings and magnitudes of the flushing tests in Diemen-Noord is provided in Table 15.

Table 15: Characteristics of the flushing tests performed in Diemen-Noord.

Locatie	Adres	Benodigde Volume- stroom m <sup>3</sup> /h	Start Datum - tijd	Eind Datum	Gem m <sup>3</sup> /h
DI 01	Hofstedenweg 54	8	24-02-2020 10:28	26-02-2020 14:25	8.15
DI 10	Parelmoervlinder 8	6	26-02-2020 16:12	28-02-2020 09:03	5.82
DI 10	Parelmoervlinder 8	6	28-02-2020 09:15	02-03-2020 08:33	6.31
DI 08	Klipperweg 101	8	02-03-2020 09:26	04-03-2020 08:19	8.12
DI 09	Agaatvlinder 35	6	04-03-2020 09:29	06-03-2020 08:18	6.04
DI 04	Wulp 34-36	6	06-03-2020 08:58	09-03-2020 08:17	5.91

Although at a first glance, it seems that the leak detection for the Diemen-Noord data was completely unsuccessful, closer analysis shows that this is actually not the case at all. We note that the experiments performed in Diemen-Noord consisted of a very close succession of flushing events with in most cases less than an hour of undisturbed signal in between. The set of experiments has been identified as a single block, and correctly so (from the first full day after the start to the last full day before the end because of the time resolution of the CFPD method), see Figure 34. Also, several of the undisturbed short periods between flushing experiments have been identified as anomalous. We must note however, that similar detections have been made at similar hours on days on which there was no flushing experiment switch. We therefore have to hypothesize that these detections are potentially related to morning peak events rather than the flushing experiments.

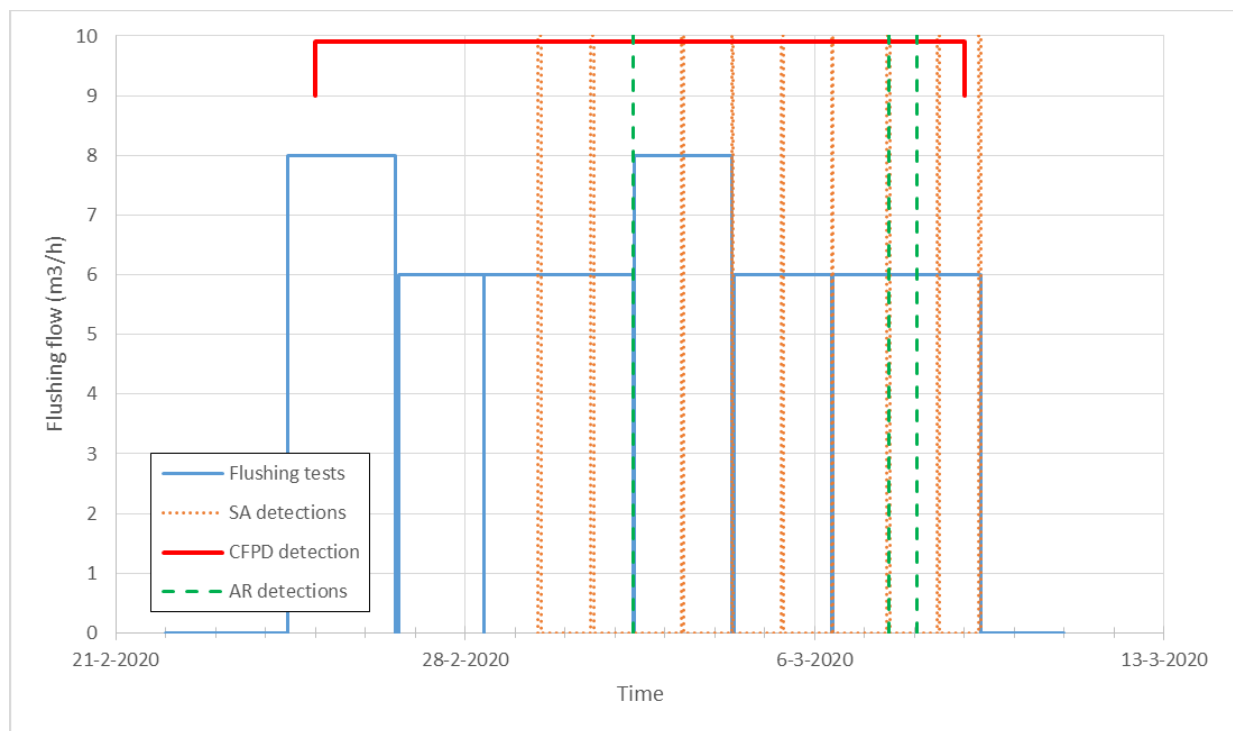


Figure 34: Coincidence of flushing experiments and detection results.

### 6.5 Additional a posteriori analyses

This section describes analysis which have been performed after knowledge of the actual flushing experiment characteristics (timings, locations, magnitudes) had been shared.

#### 6.5.1 Localization of simulated leaks in Duindorp

Because of the failure to accurately localize leakages in the Duindorp model, as described above, an attempt was made to localize leakages in a situation where the hydraulic model is more representative of the actual situation, in particular concerning demand. This was achieved in the following way:

1. simulating leakages in the hydraulic model with the same location, characteristics and timing as the flushing experiments (see Box 1);
2. generating flow and pressure time series from the model with the simulated leakage;
3. adding 0-10% noise to the signals thus obtained;
4. subjecting these flow and pressure signals thus obtained as if they were measured signals and performing the leak detection and localization analysis on them.

This was done for leakages 1, 2, 4, and 5. The results are summarized in Table 16. These all represent nodes with the smallest difference between predicted and "observed" pressures at the pressure sensor nodes. All are within an acceptable distance of the actual simulated leak; several are even spot on. Also at higher noise levels up to 10%, the results are often within 100 m of the actual leakage node. This demonstrates that when the hydraulic model used is sufficiently representative of the study area, the leak localization as implemented in Callisto can perform quite well. It also suggests that the stochastic nature of demand may not significantly incapacitate this method for leak localization without actually including stochastic demand.

Table 16: Overview of leak localization results for simulated leakages corresponding to the flushing tests described above for Duindorp. The magnitude represents the leakage coefficient, as described in Box 1.

Leak	Simulated leak			Leak localization		
	location (node)	magnitude	noise level	location (node)	magnitude	distance

1	K278714285DEH	0.74 (4 m <sup>3</sup> /h)	0%	K278714285DEH	0.760	0 m (correct node)
			2.5%	K1701255DEH	1.08	~255 m
			5%	K278714285DEH	0.787	0 m (correct node)
			10%	L120228443DEH	0.963	~60 m
2	K350840748DEH	10 (100 m <sup>3</sup> /h)	0%	K350840748DEH	10.22	0 m (correct node)
			2.5%	K350840748DEH	10.26	0 m (correct node)
			5%	K350840748DEH	10.29	0 m (correct node)
			10%	No19	12.43	~330 m
4	K278714285DEH	0.72 (4 m <sup>3</sup> /h)	0%	B240961621DEH	0.731	~23 m
			2.5%	L260302517DEH	0.775	~73 m
			5%	K250244800DEH	0.651	~8 m
			10%	K250244928DEH	0.689	~158 m
5	B240961613DEH	0.723 (4 m <sup>3</sup> /h)	0%	B1180686DEH	0.956	~103 m
			2.5%	K260302555DEH	0.775	~67 m
			5%	K260465798DEH	0.732	~4 m
			10%	L260480761DEH	0.761	~3 m
5*	B240961613DEH	0.723 (4 m <sup>3</sup> /h)	0%	B240961613DEH	0.738	0 m (correct node)
			2.5%	L260480761DEH	0.728	~3 m
			5%	L260480761DEH	0.736	~3 m
			10%	L260480751DEH	0.758	~20 m

### 6.5.2 Localization of simulated leaks in Diemen-Noord

Localization of leaks in a network model based on measurement becomes more difficult as the number of sensors becomes smaller, or said differently, more locations that provide measurements in the network (either flow or pressure) give more information to the localization algorithm for successful leak location identification. In order to demonstrate this principle, a number of localization tests were performed based on simulated leakages in the hydraulic model (modelled on the flushing experiments) with additional (virtual) sensors. In addition to the flow sensors at the two inflows, two virtual pressure sensors were included, see Figure 35.

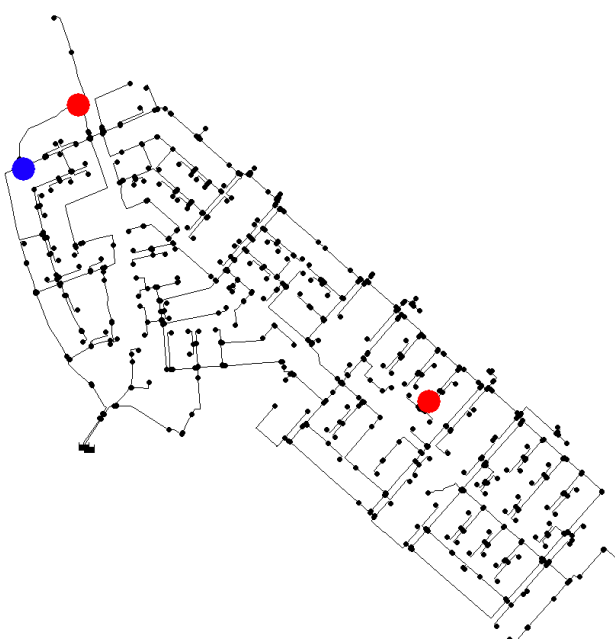


Figure 35: Locations of virtual pressure sensors used in the a posteriori simulated leak localization (red) and simulated leak (blue).

The results are presented in Table 17. In the first case, only pressure data were used. In the second, flow and pressure data were combined. Even though both perform very well, the former is spot on, the latter just one node (13 m) removed from the true location. In this case, it seems that the pressure data provide more discriminative power than the flow data, probably because of the flow sensors are very close together in the network (inflow at the lower left), in contrast to the spacing of the virtual pressure sensors.

*Table 17: Overview of leak localization results for simulated leakages corresponding to the flushing tests described above for Diemen-Noord. The magnitude represents the leakage coefficient, as described in Box 1.*

<i>Leak</i>	<i>Simulated leak</i>			<i>Leak localization</i>		
	<i>location (node)</i>	<i>magnitude</i>	<i>noise level</i>	<i>location (node)</i>	<i>magnitude</i>	<i>distance</i>
DI01 (pressure only)	A044814	1.568 ( 8.15 m <sup>3</sup> /h)	5%	A044814	1.691 (8.79 m <sup>3</sup> /h)	0 m (correct node)
DI01 (pressure + flow)	A044814	1.568 ( 8.15 m <sup>3</sup> /h)	5%	A044815	1.491 (7.75 m <sup>3</sup> /h)	13 m

# 7 Conclusions and recommendations

## 7.1 Conclusions

The Callisto project has resulted in a software tool, also named Callisto, that performs both leak detection and leak localization. Four different algorithms have been implemented for detection, and one for localization.

The tool has been tested with synthetic data and with simulated leaks (flushing) in two different DMA's in the Netherlands. This has demonstrated that the tool functions correctly and is capable of indicating the correct area for the leaks (usually within 100-200 meters from the actual leak). This holds up for significant noise levels (up to 10%), which can be considered to represent both measurement noise and effects of stochastic water demand.

Flushing experiments were performed to simulate leakages in the field, in order to challenge the Callisto tool with field data with known events. The occurrence of potential leakage events was correctly flagged by the different leak detection methods for the Duindorp case study data. Unfortunately, the tool did not succeed in correctly localizing the leaks in the Duindorp case study. Two factors are probably important in the explanation of this failure: 1) a large deviation between the hydraulic model and the actual hydraulic situation in the field, and 2) inadequate constraints on the leakage magnitude and timing from a less than rigorous analysis and identification of the leak signal.

The flushing experiments in Diemen-Noord were performed in a contiguous way, i.e. with in most cases less than an hour between consecutive flushing tests. As a result, the complete set of tests was identified as a single event (on correct days). Several of the short undisturbed periods between the flushing events were recognized by two of the methods, even though this may be coincidental and related to the particular timing of the flushing test switches. No successful localization of the flushing test was achieved. This can be ascribed to 1) large discrepancies between the hydraulic model and the actual hydraulic situation in the field and 2) the proximity of the two flow sensors. However, in an a posteriori simulation, which included two additional (virtual) pressure sensors in the network, the location of the simulated leak was correctly determined by the tool.

The basic tenet of the Callisto tool is that a combination of methods results in greater confidence in the actual detection of leaks. This has not been demonstrated conclusively so far, but the preliminary analysis presented in this report does suggest added value in the combined application of multiple methods.

## 7.2 Recommendations

The following recommendations can be made with respect to the application of the Callisto tool:

- For leak detection, perform a rigorous analysis using the Callisto tool that identifies both the timing and the magnitude of the leaks. The former is identified by all implemented methods, the latter in particular also by CFPD and spectral analysis.
- For leak localization, take care that the hydraulic model that is used is sufficiently representative of the actual hydraulic conditions in the field, both in terms of topology/connectivity and in particular also in terms of demand. The results of this project do not allow us to state which degree of representativeness is required. However, care should be taken that deviations such as significant underestimation of demand and inaccurate sensor locations in the models are prevented.

Further research and development are also recommended, to start with:

- a more rigorous analysis of the conditions under which the detection and localization algorithms perform well and under which conditions they degrade;
- broader application to more data sets to gain experience;
- an analysis of the occurrence of false positive and false negative leakage flaggings in individual methods using the combined analysis in the Callisto tool;
- analysis of flushing tests with an adequately representative hydraulic model;
- analysis of historic flow and pressure data with known leakage events in combination with an adequately representative hydraulic model.



## 8 Bibliography

- Aksela, K., Aksela, M., & Vahala, R. (2009). Leakage detection in a real distribution network using a Self-Organizing Maps. *Urban Water*, 279-289.
- Alegre, H., Baptista, J. M., Jr., E. C., Cubillo, F., Duarte, P., Hirner, W., . . . Parena, R. (2006). *Performance Indicators for Water Supply Services (Manual of Best Practice)*. IWA Publishing. Retrieved from <https://www.amazon.com/Performance-Indicators-Supply-Services-Practice/dp/1843390515?SubscriptionId=AKIAIOBINVZYXZQZ2U3A&tag=chimbori05-20&linkCode=xm2&camp=2025&creative=165953&creativeASIN=1843390515>
- Bakker, M. (2014). *Optimised control and pipe burst detection by water demand forecasting*. Ph.D. dissertation, Tu Delft. doi:10.4233/uuid:8d030ba9-da22-46d3-a018-f5d502e8d1d1
- Bakker, M., Vreeburg, J. H., Roer, M. V., & Rietveld, L. C. (2014, 9). Heuristic burst detection method using flow and pressure measurements. *Journal of Hydroinformatics*, 16, 1194-1209. doi:10.2166/hydro.2014.120
- Berardi, L., & Giustolisi, O. (2016, 5). Special Issue on the Battle of Background Leakage Assessment for Water Networks. *Journal of Water Resources Planning and Management*, 142, C2016001. doi:10.1061/(asce)wr.1943-5452.0000667
- Buchberger, S. G., & Nadimpalli, G. (2004, 7). Leak Estimation in Water Distribution Systems by Statistical Analysis of Flow Readings. *Journal of Water Resources Planning and Management*, 130, 321-329. doi:10.1061/(asce)0733-9496(2004)130:4(321)
- Caputo, A. C., & Pelagagge, P. M. (2002, 11). An inverse approach for piping networks monitoring. *Journal of Loss Prevention in the Process Industries*, 15, 497-505. doi:10.1016/s0950-4230(02)00036-0
- Caputo, A. C., & Pelagagge, P. M. (2003, 6). Using neural networks to monitor piping systems. *Process Safety Progress*, 22, 119-127. doi:10.1002/prs.680220208
- Colombo, A. F., Lee, P., & Karney, B. W. (2009, 4). A selective literature review of transient-based leak detection methods. *Journal of Hydro-environment Research*, 2, 212-227. doi:10.1016/j.jher.2009.02.003
- Deb, K., & Tiwari, S. (2008). Omni-optimizer: A generic evolutionary algorithm for single and multi-objective optimization. *European Journal of Operational Research*, 10.1016/j.ejor.2006.06.042.
- Eliades, D. G., & Polycarpou, M. M. (2012, 10). Leakage fault detection in district metered areas of water distribution systems. *Journal of Hydroinformatics*, 14, 992-1005. doi:10.2166/hydro.2012.109
- EU. (2015). *Reference Document Good Practices on Leakage Management WFD CIS WG PoM*. Office for Official Publications of the European Communities, Luxembourg.
- Geiger, G. (2006). *State of the Art in Leak Detection and Localisation*. Proc. Pipeline Technology Conference.
- Giustolisi, O., Berardi, L., Laucelli, D., Savic, D., & Kapelan, Z. (2016, 5). Operational and Tactical Management of Water and Energy Resources in Pressurized Systems: Competition at WDSA 2014. *Journal of Water Resources Planning and Management*, 142, C4015002. doi:10.1061/(asce)wr.1943-5452.0000583
- Hirsch, R. M., and J. R. Slack (1984). A Nonparametric Trend Test for Seasonal Data With Serial Dependence, *Water Resour. Res.*, 20(6), 727-732, doi:10.1029/WR020i006p00727.
- Housh, M., & Ohar, Z. (2017, 8). Multiobjective Calibration of Event-Detection Systems. *Journal of Water Resources Planning and Management*, 143, 06017004. doi:10.1061/(asce)wr.1943-5452.0000808
- Housh, M., & Ohar, Z. (2018, 8). Model-based approach for cyber-physical attack detection in water distribution systems. *Water Research*, 139, 132-143. doi:10.1016/j.watres.2018.03.039
- Hutton, C. J., Kapelan, Z., Vamvakieridou-Lyroudia, L., & Savić, D. (2014, 11). Application of Formal and Informal Bayesian Methods for Water Distribution Hydraulic Model Calibration. *Journal of Water Resources Planning and Management*, 140, 04014030. doi:10.1061/(asce)wr.1943-5452.0000412

- Li, R., Huang, H., Xin, K., & Tao, T. (2014, 12). A review of methods for burst/leakage detection and location in water distribution systems. *Water Science and Technology: Water Supply*, 15, 429-441. doi:10.2166/ws.2014.131
- Meseguer, J., Mirats-Tur, J.M., Cembrano, G., Puig, V., Quevedo, J., Pérez, R., Sanz, G., and Ibarra, D. (2014) Model-driven software tool for on-line leakage localization. Proceedings of the Water Loss Europe Conference 2014.
- Mesman, & Thienen, P. (2015). Lekzoeken met hydraulische modellen. Tech. rep., KWR Watercycle Research Institute. BTO 2015.064
- Morley, M., & Tricarico, C. (2008). Pressure driven demand extension for EPANET (EPANETpdd). Technical Rep. 2008-02. Exeter, U.K.: Centre for Water Systems, Univ. of Exeter.
- Morley, M., & Tricarico, C. (2016). Hybrid Evolutionary Optimization/Heuristic Technique for Water System Expansion and Operation. *Journal of Water Resources Planning and Management*, 142(5), 10.1061/(asce)wr.1943-5452.0000594.
- Mounce, S. R., & Machell, J. (2006). Burst detection using hydraulic data from water distribution systems with artificial neural networks. *Urban Water Journal*, 3, 21-31. doi:10.1080/15730620600578538
- Mounce, S. R., Mounce, R. B., & Boxall, J. B. (2011). Novelty detection for time series data analysis in water distribution systems using Support Vector Machines. *Journal of Hydroinformatics*, 13, 672–686. doi:10.2166/hydro.2010.144
- Mounce, S. R., Mounce, R. B., Jackson, T., Austin, J., & Boxall, J. B. (2014). Pattern matching and associative artificial neural networks for water distribution system time series data analysis. *Journal of Hydroinformatics*, 16, 617-632. doi:10.2166/hydro.2013.057
- Mounce, S., Mounce, R., & Boxall, J. (2011). Novelty detection for time series data analysis in water distribution systems using Support Vector Machines. *Journal of Hydroinformatics*, doi: 10.2166/hydro.2010.144.
- Mutikanga, H. E., Sharma, S. K., & Vairavamoorthy, K. (2013, 3). Methods and Tools for Managing Losses in Water Distribution Systems. *Journal of Water Resources Planning and Management*, 139, 166-174. doi:10.1061/(asce)wr.1943-5452.0000245
- Page, E. (1954). CONTINUOUS INSPECTION SCHEMES. *Biometrika*, Volume 41, Issue 1-2, 100–115.
- Palau, C. V., Arregui, F. J., & Carlos, M. (2012). Burst detection in water networks using principal component analysis. *Journal of Water Resources Planning and Management*, 138, 47-54. doi:10.1061/(ASCE)WR.1943-5452.0000147
- Puust, R., Kapelan, Z., Savic, D. A., & Koppel, T. (2010, 2). A review of methods for leakage management in pipe networks. *Urban Water Journal*, 7, 25-45. doi:10.1080/15730621003610878
- Quintiliani, C. and Castro Gama, M. (2020) Callisto - Comparison and joint Application of Leak detection and Localization Tools. Instruction manual, KWR 2021.002
- Romano, M., Kapelan, Z., & Savic, D. A. (2014). Automated detection of pipe bursts and other events in water distribution systems. *Journal of Water Resources Planning and Management*, 140, 457-467. Retrieved from [http://ascelibrary.org/doi/abs/10.1061/\(ASCE\)WR.1943-5452.0000339](http://ascelibrary.org/doi/abs/10.1061/(ASCE)WR.1943-5452.0000339)
- Romano, M., Woodward, K., & Kapelan, Z. (2017). Statistical Process Control Based System for Approximate Location of Pipe Bursts and Leaks in Water Distribution Systems. *Procedia Engineering*, 186, 236-243. doi:<https://doi.org/10.1016/j.proeng.2017.03.235>
- Rossman, L. (2000). EPANET 2: Users Manual. EPA/600/R-00/057 . U.S. Environmental Protection Agency, Washington, D.C.
- U.S.-EPA. (2012). CANARY version 4.3.2. Washington, DC: U.S. Environmental Protection Agency, EPA/600/R-08/040B.
- van Thienen, P. (2013, 1). A method for quantitative discrimination in flow pattern evolution of water distribution supply areas with interpretation in terms of demand and leakage. *Journal of Hydroinformatics*, 15, 86-102. doi:10.2166/hydro.2012.171
- van Thienen, P., & Vertommen, I. (2015, 11). Automated feature recognition in CFPD analyses of DMA or supply area flow data. *Journal of Hydroinformatics*, 18, 514-530. doi:10.2166/hydro.2015.056

- van Thienen, P., Pieterse-Quirijnse, I., Kater, H. D., & Duifhuizen, J. (2012). Nieuwe lekverliesbepalingsmethoden voor het drinkwaterdistributienet. H2O.
- Van Vossen-Van den Berg, J. (2017). Overzicht en toepassing van lekopsporingstechnieken. Tech. rep., KWR Watercycle Research Institute.
- Vries, D., van den Akker, B., Vonk, E., de Jong, W., & van Summeren, J. (2016). Application of machine learning techniques to predict anomalies in water supply networks. *Water Science and Technology - Water Supply*, doi: 10.2166/ws.2016.062.
- Wang, G., Dong, D., & Fang, C. (1993). Leak detection for transport pipelines based on autoregressive modeling. *IEEE Transactions on Instrumentation and Measurement*, 42, 68-71. doi:10.1109/19.206686
- Wu, Y., & Liu, S. (2017, 2). A review of data-driven approaches for burst detection in water distribution systems. *Urban Water Journal*, 14, 972-983. doi:10.1080/1573062x.2017.1279191
- Ye, G., & Fenner, R. (2010). Kalman filtering of hydraulic measurements for burst detection in water distribution systems. *ASCE Journal of Pipeline Systems Engineering and Practice*, 2. doi:10.1061/(ASCE)PS.1949-1204.0000070

# I Appendix: Flushing plan and proposed leakage locations to water companies.



## Memo

**Van**  
Mario Castro-Gama

**Onderwerp**  
TKI CALLISTO Spuiplan

**Datum**  
21 oktober 2019

**Bestemd voor**  
Arne Bosch – Waternet  
Michael van den Boom - Dunea

**Kopie / afschrift**

**Pagina**  
1/11

## TKI CALLISTO

Binnen het TKI project Callisto worden lekkages gesimuleerd door op verschillende brandkranen (BK) een bekende volumestroom te onttrekken. Deze volumestromen worden gedurende twee dagen onttrokken waarbinnen de metingen in het net plaatsvinden.

De gebieden waar binnen de lekkages gesimuleerd worden staan in **Error! Reference source not found.** Er zijn twee gebieden voor Waternet en een gebied voor Dunea gedefinieerd.

Binnen ieder gebied zijn door het waterleidingbedrijf de brandkranen geselecteerd waarop de simulatie kan plaatsvinden, zie Tabel 2, Tabel 3 en Tabel 4

Tabel 1. Overzicht van gebieden (DMA) voor elke drinkwaterbedrijf

Waterbedrijf	DMA	Aantal BK	aantal BK simulatie
Waternet	Diemen-Noord	136	10
Waternet	Heemstede	843	12
Dunea	Duindorp	91	10

Tabel 2. Lijst van geselecteerde brandkranen voor Waternet - Diemen Noord

Locatie DI	asset_id	x	y	ground_lev	Diameter brandkraan	adres	opmerking	Diameter leiding
DI 01	673664	126453.31	485054.05	-1.6	80	Hofstedenweg 54 DIEMEN	rechts draaiend	118
DI 02	269798	126680.50	485122.18	-1.79	80	Diemzigt 68 DIEMEN	rechts draaiend	118
DI 03	631749	126827.28	484742.67	-1.79	80	Leeuwerik 10 DIEMEN	rechts draaiend	103 & 32
DI 04	273063	126962.20	484973.78	-1.79	80	Rietzangerweg 120 DIEMEN	rechts draaiend	118
DI 05	270543	127039.51	484753.93	-1.79	80	Kolgans 106 DIEMEN	rechts draaiend	118
DI 06	271398	127144.14	484494.91	-1.79	80	Schouw 26 DIEMEN	rechts draaiend	118
DI 07	292379	127226.08	484812.16	-1.79	80	Botterweg 129 DIEMEN	rechts draaiend	255 & 235
DI 08	292451	127353.11	484612.58	-1.89	80	Klipperweg 101 DIEMEN	rechts draaiend	118
DI 09	289720	127438.10	484308.35	-1.79	80	Agaatvlinder 35 DIEMEN	rechts draaiend	40
DI 10	291132	127590.49	484398.02	-1.79	80	Heivlinderweg 77 DIEMEN	rechts draaiend	235

Tabel 3. Lijst van brandkranen voor Waternet - Heemstede



Locatie	Asset_id	x	y	ground_lev	Diameter Brandkraan	Adres	Opmerking	Diameter Leiding
HE 01	270019	101512.55	484357.78	0.5	80	Amstellaan 13 HEEMSTEDE	onbekend	49
HE 02	677431	101677.60	483699.48	-0.2	80	Herenweg 27 HEEMSTEDE	rechts draaiend	142
HE 03	273558	101823.52	482467.79	0.6	80	Korhoenlaan 19 HEEMSTEDE	onbekend	80 & 49
HE 04	273266	101830.79	485121.14	0.5	80	Van der Waalslaan 31 HEEMSTEDE	onbekend	200
HE 05	272075	102079.69	486024.62	0.6	80	Zandvoortselaan 76 HEEMSTEDE	onbekend	103
HE 06	273477	102253.24	482824.91	0.6	80	Troelstralaan 35A HEEMSTEDE	onbekend	103
HE 07	272662	102541.50	483202.65	-0.3	80	Aletta Jacobslaan 22 HEEMSTEDE	onbekend	100
HE 08	270410	102560.00	484194.99	0.7	80	Groenendaalkade 2 HEEMSTEDE	onbekend	80
HE 09	271366	102679.92	485576.93	0	80	Wasserij-Annalaan 209 HEEMSTEDE	onbekend	100
HE 10	645308	102820.65	484942.70	0.6	80	Binnenweg 2 HEEMSTEDE	rechts draaiend	49
HE 11	273252	103410.33	483903.93	0.2	80	Slotlaan 15B HEEMSTEDE	onbekend	100
HE 12	272658	103696.15	485888.75	0.6	80	H W Mesdaglaan 34 HEEMSTEDE	onbekend	100

Dunea heeft 91 brandkranen in Duindorp, maar er zijn er slechts 41 operationeel. Van die operationele groep zijn 10 locaties voorgesteld.

Tabel 4. Lijst van brandkranen voor Dunea - Duindorp

Locatie DU	NUMMER	x	Y	MEETMETHOD	AFSLUITSEC	NADERE_POS (Adres)	FUNCTIE	Diameter Brandkraan
DU 01	11282	77359.55	456080.11	Digitaal (gps)	6035550	Schouwensestraat 5	Spuibrandkraan	104.6
DU 02	11277	77462.86	456180.61	Digitaal (gps)	6928826	Pluivierstraat 409	Spuibrandkraan	104.6
DU 03	11276	77556.27	456104.35	Digitaal (gps)	6929006	Breezandstraat 1	Spuibrandkraan	104.6
DU 04	11427	77773.14	457058.70	Digitaal (gps)	6003548	Boeistraat 40	Spuibrandkraan	70 & 46
DU 05	11250	77987.38	456742.29	Digitaal (gps)	6004190	Kranenburgweg 260	Spuibrandkraan	96
DU 06	8805	77794.16	456548.99	Analoog	6004322	Terschellingsestraat 91	Brandkraan	104.6
DU 07	2962	77558.96	456485.23	Analoog	6004372	Markensestraat 135	Brandkraan	100
DU 08	9672	77827.79	456654.70	Analoog	7862962	Zeezwaluwstraat 92	Brandkraan	104.6
DU 09	10968	77711.13	456809.43	Digitaal (gps)	6004120	Zeezwaluwstraat 281	Brandkraan	65
DU 10	9622	77942.00	456545.31	Analoog	7049760	Meeuwenstraat 8-d	Brandkraan	104.6 & 59



\*\*De eindselectie/eindbeslissing van de brandkranen/locaties om te spuien wordt door elk drinkwaterbedrijf zelf gemaakt. Dit zullen er vijf of zes zijn, afhankelijk van de mogelijkheden voor de inzet van het waterleidingbedrijf \*\*

Elke spui zal twee dagen duren. De doorlooptijd bedraagt één maand en zonder weekenddagen kunnen vijf of zes lekken gesimuleerd worden.

## 1 AFBAKENING SPUIGEBIED

1. Rekenkundig vaststellen met een leidingnetmodel wat de consequentie is (drukken en volumestromen) van de gesimuleerde lekkage (spuiactie).
2. Vaststellen of de optredende extra snelheid in de leidingen tot een (bruin water) probleem kunnen leiden
3. Indien de aanvoerleidingen gespuid gaan worden:  
Vergunningen aanvragen?  
Brandkranen (zie de kaart, voor elk gebied zijn locaties gesuggereerd)
4. Uitvoeren spui activiteit begeleid met volume- en drukmetingen (loggers)

## 2 Voorbereiden spuiacties Diemen Noord, Heemstede en Duindorp

1. Opstellen spui-model Diemen-Noord en Heemstede
2. Spuiacties plannen, intern bij drinkwaterbedrijf  
Spuien moet PraktijkCode Drinkwater 2-2015 volgen (KWR | PCD 2:2015 )  
Locaties - "wish list")  
Eindselectie van drinkwaterbedrijf  
Controle van spuien.  
Spui-punten plaatsen voor grote volumestromen.
3. Protocol opstellen  
Voor de betreffende brandkraan de volumestroom bepalen  
Vaststellen hoe deze volumestroom aangebracht zal worden (kaliberplaten of volumestroommeting met regelafsluiter)  
Volumestroommeters (loggers, voor het vastleggen van de actie)  
Drukmetingen (optioneel)
4. Uitvoeren spuiacties  
Opgesteld spuiplan doorlopen  
Registratie volumestromen  
Registratie naast de brandkranen (druk als mogelijk).  
Registratie bijzonderheden. Het is mogelijk dat er klachten van klanten optreden en andere operaties (afsluiters of leidingen gesloten zijn) in andere locaties  
Voor elke spui-actie is een termijn van 5 dagen voldoende.  
  
Drinkwaterbedrijf zal een Memo voor KWR opstellen  
Datum spuiactie



Tijdsreeksen van de DMA invoer. Als mogelijk data elke minuut of elke, en voor Duindorp is bekend dat data is elke kwartier. Afhankelijk van aantal. Het is verwacht dat binnen een maand vijf of zes lekkages zijn gesimuleerd.

#### A. De noodzakelijke acties op korte termijn bij het drinkwaterbedrijf

Vergunningen voor werkzaamheden moeten worden voorbereid.

communicatie met klanten dichtbij de spuilocaties

Interne communicatie met monteurs (field operators)

- Overleg met spuiplanner van verwachte resultaten
- Misschien zijn sommige locaties niet beschikbaar, de selectie moet op korte termijn gebeuren. Selectie vindt plaats door drinkwaterbedrijf,
- De mogelijkheid bestaat dat met de simulatie een watersnelheid bereikt wordt waarbij sediment wordt opgewerveld. Als dit tot kwaliteitsproblemen kan leiden moet de locatie wellicht van te voren worden schoongemaakt door middel van een gerichte beperkte spuiactie.
- Vaststellen noodzakelijke spuiacties transportleidingen (kan ook "geen" zijn)

#### B. Acties tijdens de spuien

Het drinkwaterbedrijf heeft al wat locaties geselecteerd. Er is een volumestroom voor elke combinatie van diameter, zie Tabel 5, voor water snelheid van 0,20 m/s.

Diameter Leiding (mm)	Volumestroom (m <sup>3</sup> /uur)
45	1.15
59	1.97
75	3.18
100	5.65
125	8.84
150	12.72
200	22.62
250	35.34

Tabel 5. Volumestromen bij het uitvoeren van een leiding met 0,20 m/s bij verschillende diameters. De leiding heeft een druk van 30 mwk.

#### Leidingnet

Voor het toepassen van de lekkages moeten de diameter, en de te openen brandkranen bekend zijn. De keuze om de benodigde volumestroom als extra aan te brengen op een bestaande volumestroom hangt sterk af van de lokale situatie.

#### Metingen - Volumestroom



Voor de meting van de volumestroom over de brandkraan zijn verschillende mogelijkheden. De volumestroom kan worden afgeleid van een gemeten snelheid in de standpijp van de brandkraan waarop de meting wordt uitgevoerd. De volumestroom kan op verschillende wijzen worden gemeten:

- (i) Electromagnetische 'clamp on' meter op de uitstroom van de brandkraan;
- (ii) met een insteekmeter op de standpijp waarmee de watersnelheid direct wordt gemeten via een ingestoken schoepenrad of,
- (iii) een opzetstuk met een ingebouwde volumestroommeter.

Door het opzetstuk op de brandkraan uit te voeren met een volumestroombegrenzer (kaliberplaat) wordt een te grote volumestroom bij het openen en/of schoonspoelen van de brandkraan voorkomen. Een kaliberplaat heeft ook als voordeel dat de volumestroom redelijk constant blijft gedurende de proef

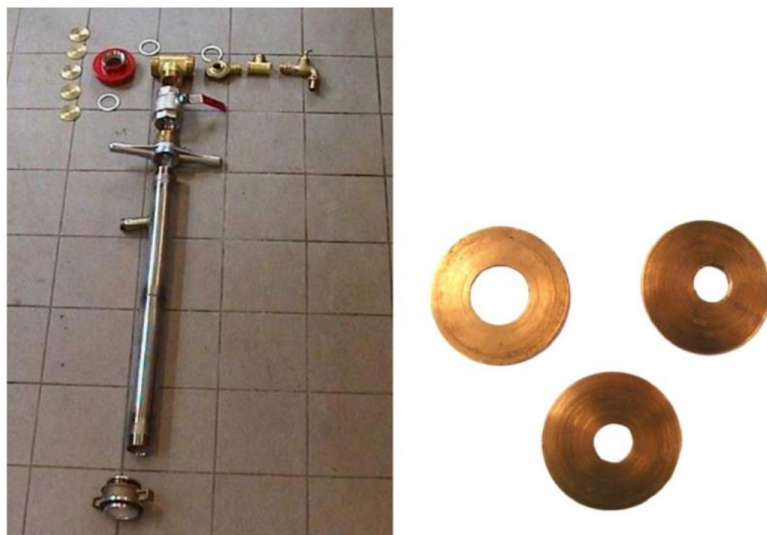
Voor de metingen is een datalogger aan te bevelen. De volumestroom kan binnen de dag veranderen.

#### **Brandkraan met toebehoren**

Een meting volgens de spuien wordt uitgevoerd over een bestaande brandkraan. Een dergelijk meetpunt (Figuur 1), kan worden voorzien van het volgende instrumentarium:

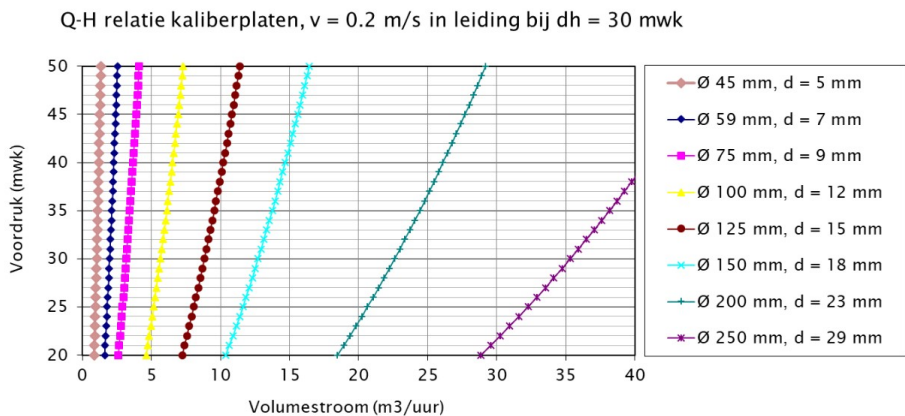
- Afsluiter;
- Volumestroombegrenzer; Door een kaliberplaat toe te passen, hoeft de volumestroom niet te worden geregeld met de afsluiter. De kaliberplaat voorkomt een 'overshoot' bij het openen van de brandkraan. Een kaliberplaat heeft slechts een beperkt gebied in drukverlies waarin deze correct is. Als er grote verschillen in druk bestaan tussen diverse voorzieningsgebieden moeten voor elk gebied 'eigen' kaliberplaten worden gebruikt. In Bijlage II is het resultaat opgenomen van een theoretische benadering van dergelijke kaliberplaten.
- Drukopnemer (optioneel);
- Volumestroommeter (optioneel).





Figuur 1. Standpijp voor een brandkraan voor een spuien met mogelijkheid voor een insteekmeter (volumestroom), kogelafsluiter, monsterkraan en kaliberplaten voor het beperken van de volumestroom van het gesimuleerde lek (herkomst foto onbekend).

Het drukverlies en volumestroom zijn afhankelijk van de snelheid van water in de leiding en het diameter van de brandkraan. Voor een kwantificatie van de volumestroom voor een snelheid van 0,2 m/s zie Tabel 5. Voor verschillende kaliberplaat diameter gaten zijn verschillende volumestromen mogelijk, afhankelijk van de voordruk in de leiding (zie Figuur 6).



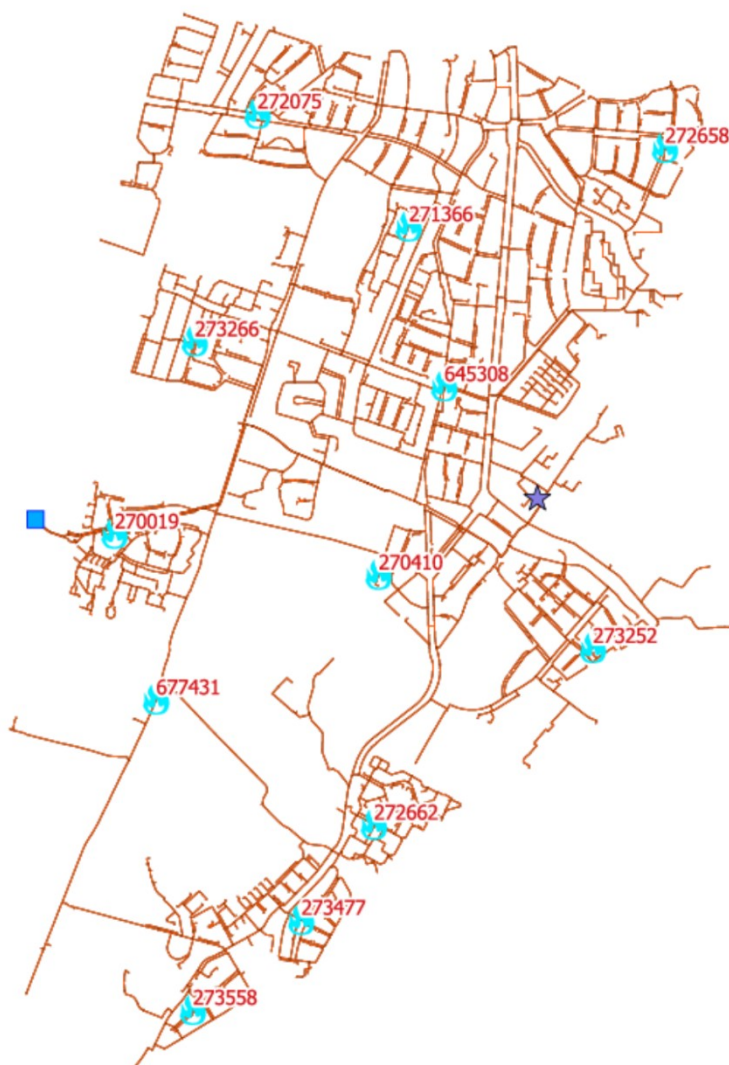
Figuur 2. Q-H relatie van kaliberplaten voor verschillende gat diameters d = 5, 7, 9, 12, 15, 18, 23, 29 mm. (spreadsheet is beschikbaar waarmee de hoeveelheid bepaald wordt).



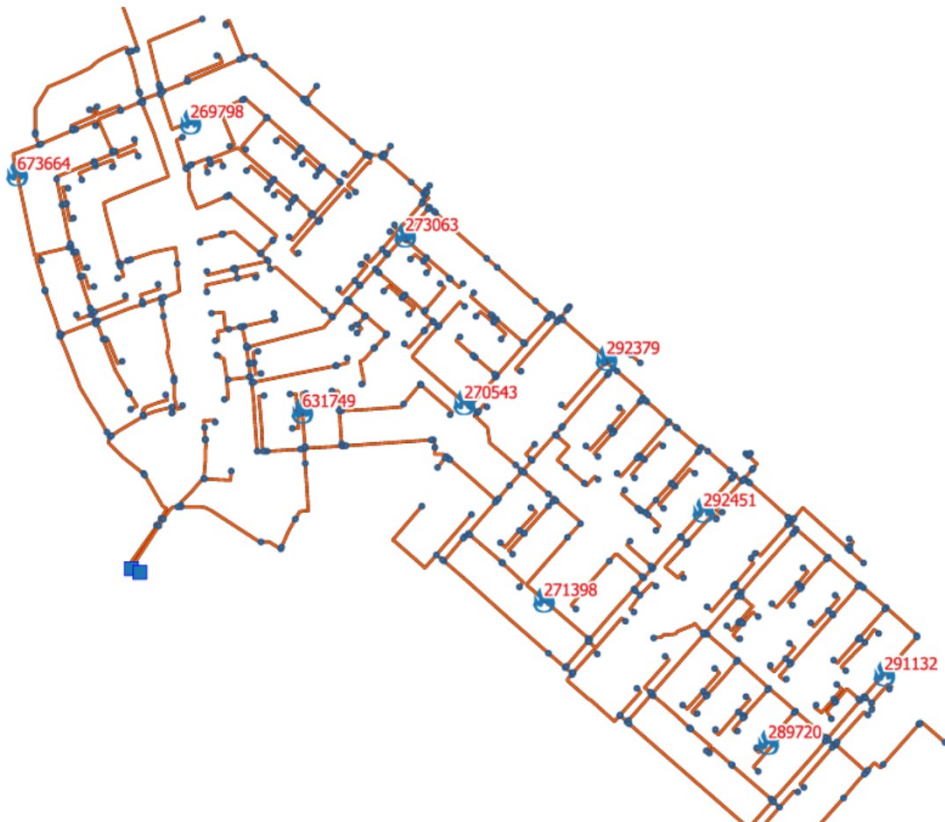
### **C. Acties na spuien korte termijn**

1. Netaanpassingen doorvoeren → terug naar normale operatie. De monteur wordt gevraagd om bijzonderheden te registreren.
2. Dataverzameling door de drinkwaterbedrijven en naar KWR sturen
3. KWR en W+B zullen de data opschonen
4. KWR en W+B - CALLISTO verzorgen de software validatie met data van spuien

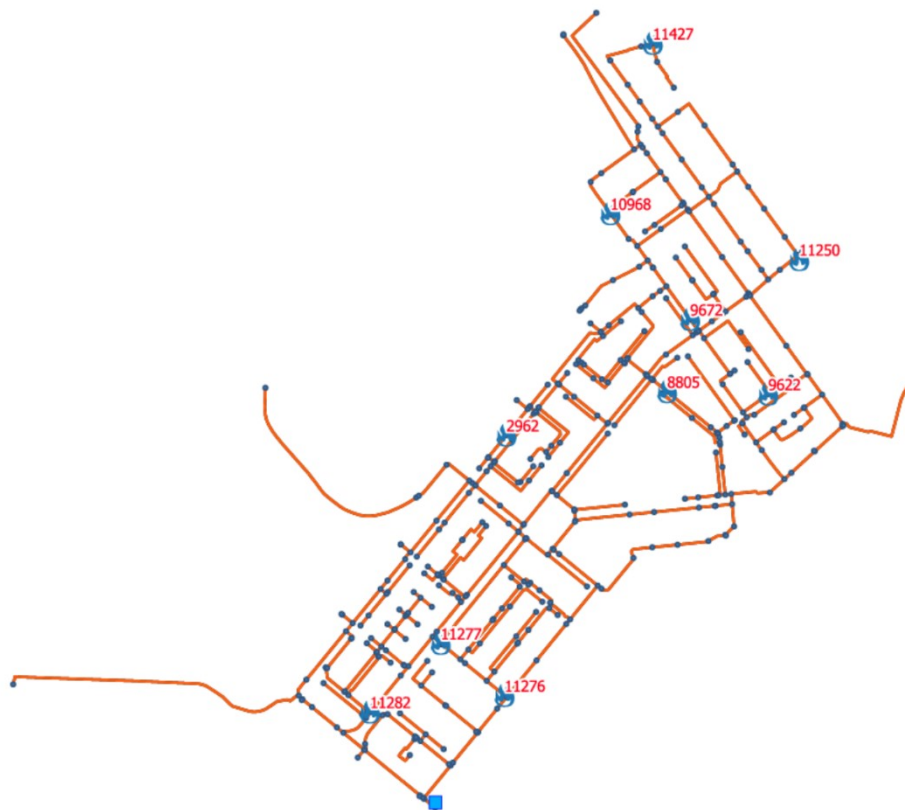
### **5. KAART PER GEBIED**



Figuur 3. Heemstede locaties



Figuur 4. Diemen Noord locaties



Figuur 5. Duindorp locaties

## 6. TYPISCHE INSTALLATIE VOORBEELD



Figuur 6. Volledig ingericht meetpunt en aangepaste fittersbus. Op het spuijpunt is vanaf de bocht de volgende apparatuur aanwezig: T-stuk met aftak naar drukopnemer en troebelheidsmeter, snelheidsmeter voor de volumestroom, afsluiter en spuizak. In de bus zijn de troebelheidsmeter, snelheidsmeter, drukregistratie en datalogger opgesteld (hoffelijkheid van foto: WML, 2014).